The Novel CircSLC6A6/miR-1265/C2CD4A Axis Promotes Colorectal Cancer Growth by Suppressing P53 Signaling Pathway

Zeyin Rong
Shanghai General Hospital
Zai Luo
Shanghai General Hospital
Zhongmao Fu
Shanghai General Hospital
Pengshan Zhang
Shanghai General Hospital
Tengfei Li
Shanghai General Hospital
Jianming Zhang
Shanghai General Hospital
Zhonglin Zhu
Shanghai General Hospital
Zhilong Yu
Shanghai General Hospital
Qi Li
Shuguang Hospital
Zhengjun Qiu
Shanghai General Hospital
Chen Huang (richard-hc@sohu.com)
Shanghai General Hospital, Shanghai Jiaotong University School of Medicine

Research Article

Keywords: C2CD4A, P53, circSLC6A6, miR-1265, CRC

Posted Date: June 22nd, 2021

DOI: https://doi.org/10.21203/rs.3.rs-628280/v1

Abstract

Background: Colorectal cancer (CRC) ranks as the third most frequently diagnosed cancer and is a leading cause of cancer-related deaths. Therefore, further researches were required to identify novel and more effective diagnoses and to identify molecular targets in treatment of CRC.

Methods: CRC fresh frozen tissues and cell lines were used to detect C2CD4A expression by qRT-PCR and western blotting. The biological functions of C2CD4A were performed in *vitro* and in *vivo*. Western blotting, cDNA array, IP-MS, Co-IP, and Ubiquitination assay were used to analyze the interaction between C2CD4A and p53. Bioinformatics analysis, FISH, RNA sequencing, luciferase reporter assay, RNA immunoprecipitation, RNA pull-down and rescue experiments, were deployed to detect upstream regulation mechanism of C2CD4A.

Results: C2CD4A was aberrantly upregulated in CRC tissues compared with adjacent normal colorectal tissues. C2CD4A knockdown significantly promoted cell apoptosis and with inhibited proliferation in *vitro*, and tumorigenicity in *vivo*, whereas C2CD4A overexpression had displayed an opposite effect. Moreover, circSLC6A6 was upregulated and positively associated with C2CD4A expression in CRC tissues. C2CD4A was positively regulated by circSLC6A6 via sponging miR-1265. Fundamentally, C2CD4A inhibited P53 signaling pathway through interacting with P53 and increasing its ubiquitination and degradation.

Conclusion: Our results identified that circSLC6A6/miR-1265/C2CD4A axis, which was involved in CRC via the P53 signaling pathway, could be as a therapeutic target for CRC.

Background

Colorectal cancer (CRC) is one of the most common cancer and a major cause of mortality and morbidity in the developed countries, and ranks as the third most frequently diagnosed cancer and is a leading cause of cancer-related deaths both in men and women worldwide [1]. Under the numerous endeavors for early diagnosis and appropriate treatments of CRC in the past few decades, early CRC survival rate has significantly improved, with five years survival rate over 90%. However, the prognosis of CRC patients with advanced metastatic was still less desirable [2, 3]. In recent years, the morbidity of CRC grew steadily in China [4], yet the molecular mechanism of CRC still remained vague [5]. Hence, more research is urgently required before final goal of working out novel and effective diagnostic methods and identifying molecular targets of CRC.

Through analysis of the CRC clinical samples from the Cancer Genome Atlas (TCGA) database, this paper presented the discovery of crucial genes related to CRC development and progression development and progression. There were 461 CRC samples with RNAseq and RNAseqV2 data, in which 50 paired samples were with pathological data and RNAseq data (41 paired samples colon adenocarcinoma samples and 9 paired rectum adenocarcinoma samples). Based on the above 50 paired CRC samples, CRC related differentially expressed genes were screened. Then, C2CD4A (C2 calcium dependent domain containing 4A) expression was found significantly higher in CRC tissues than in the paired normal

colorectal tissues (19.869 fold change, P < 0.001). The gene C2CD4A belonged to the C2CD4 family, which included 3 members, namely C2CD4A, C2CD4B and C2CD4C. Due to its high sequence similarity and coding cells nuclear protein, it was also known as the sequence similarity family 148A (FAM148A) or nuclear localization factor 1 (NLF-l) [6, 7]. The C2CD4A gene is located on the human chromosome long arm 15q 22.2, which contains 3941 base pairs, 1 intron and 2 exons. Encoded a protein containing a calcium-dependent lazy C2 domain, C2CD4A gene is a nuclear protein with a relative molecular mass of 39KDa. The encoded protein from C2CD4A gene might adhere to the cell membrane through C2 domain with a series of consequential biological effects. C2CD4A was also widely expressed in the pancreas, liver, muscle and adipose tissue of animals. A slice of change in C2 domain coming along with the variation in C2CD4A gene would affect its encoded protein structure and function. Genome-wide association studies suggested that C2CD4A was highly associated with diabetes and was rarely found in tumor cases. In other words, there were research gap in C2CD4A's role in regulating the tumorigenesis of CRC and its mechanism in affecting tumor progression.

P53, a bona fide tumor suppressor gene, was essential for genome integrity and stability [8]. As a vital gatekeeper, P53 was mutated in all sorts of cancers for which it would inhibit cell proliferation, induce cell apoptosis, cell senescence, block cell metastasis and regulate energy metabolism by P53's transcriptional activities[9]. P53 mutation was detected in over 50% cases of CRC in which the mutation frequency of P53 was positively associated with malignancy degree of CRC [10, 11]. MDM2, a transcriptional target gene of P53, possessed intrinsic E3 ubiquitin ligase activity, was directly bound to P53 and mediated its ubiquitin-dependent proteolysis through its N-terminal, and then formed a negative feedback loop with P53 [12]. Thus, direct or indirect inhibition of the MDM2 activity was crucial for P53 function. Given the critical role of P53 inactivation in the development of CRC, it was significantly important to figure out the molecular mechanism by which P53 was dysregulated in CRC. Herein, we found that C2CD4A might interact with P53 to increase P53 protein ubiquitin-degradation and thus facilitated the proliferation of CRC.

Circular RNAs (circRNAs) is an intriguing one in ncRNAs, which are formed by back-splicing or exon skipping and are characterized as covalently closed loop structures with neither 5' to 3' polarity nor a polyadenylated tail [13]. CircRNAs are insensitive to multiple exonuclease and have displayed a stable state due to its peculiar structure with the potential to be an ideal biomarker for diagnosis of cancer [14, 15]. And it has a particular cell and tissue type or developmental stage-specific expression pattern in eukaryote, and has been proven to take part in the pathology of different diseases [16]. The specificity of the circRNA structure determines its specific biological functions, such as functions in regulation of gene transcription, and protein translation [17]. CircRNAs have also been shown to function as a competing endogenous RNA (ceRNA) to compete for miRNA binding [18]. Relationships between circRNAs and diseases, especially in cancers, have recently been reported, including ones related to gastric cancer, bladder cancer, liver cancer and CRC [19–22]. It had presented an important molecular biological basis to understand the complicated cancer progression. This research found that an upregulated circRNA-hsa_circ_0004705 (termed as circSLC6A6) from the SLC6A6 gene was significantly correlated with CRC patients prognosis. It was found that circSLC6A6 was highly expressed in CRC tissues and cells.

Moreover, circSLC6A6 functioned as a sponge of miR-1265 to promote the growth of CRC by increasing the expression of C2CD4A protein and facilitating the degradation of P53 protein. Therefore, our research was the first revealed the novel circSLC6A6/miR-1265/C2CD4A/P53 axis in the CRC proliferation and its molecular mechanism to provide a promising therapeutic targets of CRC.

Materials And Methods

Cell culture and culture conditions

The human CRC (HCT116, RKO, HT29, HCT8, SW620, SW480, and LOVO), 293T and normal colon epithelial (FHC) cell lines were purchased from the Chinese Academy of Sciences, Shanghai Institutes for Biological Sciences (Shanghai, China). HCT116 p53+/+ and HCT116 p53−/− cells were obtained from American Type Culture Collection (ATCC, Maryland, USA). All these cell lines were maintained in DMEM medium supplemented with 10% FBS at standard culture conditions (5% CO2, 95% humidity and 37 °C).

Patients and tissue samples

108 paired CRC and adjacent normal tissues were collected from Shanghai General Hospital between 2013 and 2014, and were paraffin embedded for the tissue microarray (TMA) construction (the final TMA contained 106 CRC tissues and 106 adjacent normal tissues). Meanwhile, sixty-three pairs of human CRC fresh tissues and adjacent normal tissues were collected from Shanghai General Hospital after radical surgical resection between 2015 and 2017. After resection, the tissues were transported in liquid nitrogen and stored at -80°C refrigerator for RNA and protein extraction. No patients had received chemotherapy and radiotherapy before surgery. The detailed clinicopathological feature was confirmed by at least two pathologists according to the American Joint Committee on Cance (AJCC). Our research was approved by the Ethics Committee for Clinical Research of Shanghai General Hospital.

RNA extraction, gDNA extraction, and quantitative real-time polymerase chain reaction (qRT-PCR)

Total RNA was extracted from human CRC cells lines and frozen tissues with RNAiso Plus reagent (Takara, Japan) according to the manufacturer's protocol. Genomic DNA (gDNA) was extracted from tissues using Fast Pure Cell/Tissue DNA Isolation Mini Kit (Vazyme, DC102) in accordance with the manufacturer's protocol. Cytoplasmic and nuclear RNAs were separated using PARIS™ Kit (Invitrogen, USA) following the manufacturer's protocol. For circRNA and mRNA, reverse transcription was conducted using the PrimeScript RT Master Mix (Takara, Japan). For miRNA, reverse transcription was conducted using PrimeScript RT Reagent Kit (Takara, Japan) with corresponding stem-loop primers. qRT-PCR was conducted by using SYBR Green Master Mix (Yeasen, China) in line with the manufacturer's protocol on Roche real-time PCR instrument (Roche Applied Science, USA). Human GAPDH was selected as internal control for circRNAs and mRNAs. U6 was selected as internal control for miRNAs. All the primers were listed in Additional file 1: Table S1. The relative RNA expression levels were determined by the $2^{-\Delta\Delta CT}$ method. Each qRT-PCR experiment was carried out in triplicate.

Transfection, oligonucleotides and plasmids

For lentivirus transfections, short hairpin RNA (shRNA) plasmid targeting human C2CD4A and the control plasmid (sh-Ctrl) were inserted into a lentiviral vector (Genechem Shanghai, China). The sequences to knockdown human C2CD4A were showed in Additional file 2: Table S2. The human C2CD4A gene was cloned into pLVX plasmids (Genechem, Shanghai, China) to construct the C2CD4A overexpression vector. Then, the indicated cells with lentiviral transduction were selected with puromycin (Beyotime Biotechnology, China) for two weeks. The efficiency of C2CD4A knockdown and overexpression were verified by qRT-PCR and western blotting. Meanwhile, to regulate circSLC6A6, miR-1265, and MDM2 expression, oligonucleotides and plasmids were constructed. The siRNAs targeting circSLC6A6 and MDM2 were provided by GenePharma (Shanghai, China). The relevant oligonucleotides sequences were presented in Additional file 2: Table S2. Additionally, full length of circSLC6A6 was successfully cloned into the lentiviral plasmid pEX-3 (GenePharma, Shanghai, China) to establish the cell line with stable expression of circSLC6A6. The mimics, inhibitor and controls for miR-1265 were purchased from GenePharma (Shanghai, China). Cells transfection were performed using Lipofectamine 3000 (Invitrogen).

Immunohistochemistry (IHC)

The slides were incubated with primary antibodies including P53 (1:100, Abcam, USA), Cleaved-caspase3 (1:400; CST, USA), P21 (1:50, CST, USA), Bax (1:400, CST, USA), Ki-67 (1:500, Abcam, USA) at 4°C overnight, respectively, and then incubated with HRP labeled secondary antibody for 1 h at room temperature. The details about IHC staining score were shown in our previously published research [23].

Nucleic acid electrophoresis and RNase R treatment

Nucleic acid electrophoresis and RNase R treatment were performed as previously described [19, 24] .

Western blotting analysis

All cells and tissues were lysed with RIPA lysis buffer (New Cell & Molecular Biotech Co, China). Total protein concentration was measured by BCA Protein Assay Kit (Beyotime Biotechnology, China). Protein lysates (50μg) were separated in different concentrations of sodium dodecyl sulfate-polyacrylamide gels electrophoresis (SDS-PAGE) and then transferred to PVDF membranes (Millipore, Billerica, USA). The membranes were subsequently blocked in 5% non-fat milk at room temperature for 2h and then incubated at 4 °C overnight with the primary antibodies: anti-C2CD4A (1:500; Sigma-Aldrich, USA. The applications not including IHC staining), anti-Flag (1:5000; Sigma-Aldrich, USA), anti-His (1:1000; CST, USA), anti-HA (1:1000, CST, USA), anti-GFP (1:1000; Abcam, USA), anti-MDM2 (1:1000; CST, USA), anti-P53 (1:1000; Abcam, USA), anti-P21 (1:1000; CST, USA), anti-Ki67 (1:5000; Abcam, USA), anti-Bax (1:1000; CST, USA), anti-Cleaved-caspase3 (1:1000; CST, USA), anti-GAPDH (1:1000; CST, USA). Then, the membranes were incubated with appropriate secondary antibodies (1:000; CST, USA) for 2h. After

membranes being washed three times, the brands were detected using ECL chemiluminescent reagent (Millipore, MA, USA). GAPDH was used as a loading control.

Cell proliferation assay

For the cell counting kit-8 (CCK-8) (Dojindo, Japan) assay, the transduced CRC cells were seeded in 96-well microplates with 1000 cells per well in humidified air containing 5% CO2 at 37˚C. OD values at 450 nm were measured every 24 hours by Gen5 microplate reader (BioTek). For the 5-Ethynyl-2'-deoxyuridine (EdU) cell growth assay, the transduced CRC cells were seeded into 96-well microplates and cultured for 24h. Then, the cells were incubated with 50 μM EdU (RiboBio, Guangzhou, China) for 2h, then, cell nuclei were stained with Hoechst 33342 for 30 min. The percentage of EdU-positive cells was presented by: (EdU positive cells/Hoechst positive cells) ×100%. Colony formation assays were performed to evaluate the cloning capability of CRC cells, the transduced CRC cells were seeded into 6-well plates (2000 cells/well) and incubated at 37 °C to facilitate colony formation. Two weeks later, the cells were fixed in methyl alcohol for 30min and then stained with 1% crystal violet for 20min. All experiments were performed in triplicate.

Apoptosis analysis

The cell apoptosis assay was conducted by using the AnnexinV-PE/7-AAD Apoptosis Detection Kit (MultiSciences Biotech Co, Ltd) in accordance with the manufacturer's protocol [23]. The apoptotic cells rate were detected and analyzed by a flow cytometrer (BD Biosciences, San Jose, CA, USA). All experiments were performed in triplicate.

The cancer genome atlas (TCGA) database, GEPIA dataset and Oncomine database

The CRC data was downloaded from TCGA database (https://cancergenome.nih.gov).

There are 461 colon cancer samples with available data in TCGA database, including 458 RNA-seq samples, of which 41 pairs with paired sample data and pathological information. There are 171 rectal cancer samples with available data in TCGA database, of which RNA-seq samples have 166; there are 9 pairs with paired sample data and pathological information. Our expression profile analysis is based on these 50 paired samples with RNA-seq data, paired sample data and pathological information. In the above 50 pairs of CRC tissues and adjacent tissues, after filtering and screening, significantly differentially expressed genes were found. Gene Expression Profiling Interactive Analysis (GEPIA) dataset (http://gepia.cancer-pku.cn/detail.php) were used to determine the expression of C2CD4A in CRC tissues and normal tissues. Oncomine database (https://www.oncomine.org) was performed to detect the level of C2CD4A expression in CRC and normal adjacent tissues. The expression of C2CD4A mRNA was significantly higher in 45 colorectal adenocarcinoma (Skrzypczak Colorectal Statistics, 2010) and 36 colorectal carcinoma compared with normal colorectal mucosa tissues, respectively.

cDNA array analysis

cDNA array were performed as previously described to identify differentially expressed genes (DEGs) between three pairs RKO/sh-C2CD4A-1 and RKO/sh-Ctrl cells [25]. Then, Kyoto Encyclopedia of Genes and Genomes (KEGG) analysis were used to analyze the DEGs.

Animal experiments

Four-week-old male BALB/c athymic nude mice were randomly divided into 5 groups (n=5). And injected subcutaneously into subscapular with 2.0×10^6 cells from the stable transfected RKO cell lines (shCtrl, sh-C2CD4A-1, sh-C2CD4A-2) to establish the CRC cancer xenograft model, respectively. Tumor size was measured every week to monitor tumor growth. Both of minimum (Width) and maximum (Length) diameters were measured for all tumors; the tumor volumes were calculated using the formula: $0.5\times length\times width^2$. All mice were sacrificed at 38 days, and tumors were surgically removed and weighed. After fixed in 4% paraformaldehyde, all tumors were embedded in paraffin and sliced into 4μm slides for IHC staining. All animal experiments were approved by the Institutional Animal Care of Shanghai General Hospital.

Luciferase reporter assay

Luciferase plasmids (pGL3-Firefly-Renilla containing circSLC6A6 sequence or Mutant sequence, pGL3-Firefly-Renilla containing C2CD4A 3'-UTR sequence or Mutant sequence) were purchased from GenePharma (Shanghai, China) and were co-transfected with miR-1265 mimics or inhibitor to indicated cells using Lipofectamine^{TM} 2000 reagent. In short, the transfected cells were lysed with 100μl of passive lysis buffer and the supernatant was collected after centrifuge. Cell samples (20μl) and 100μl of LARII were added into 96-well luminometer plates, followed by firefly luciferase activity detection. Then, 100μl of Stop & GloR reagent was added into 96-well luminometer plates to detect Renilla luciferase activity. The ratio of firefly luciferase/Renilla luciferase activity was used to detect the effects of miR-1265 on luciferase reporter plasmids. All experiments were independently performed in triplicate.

Fluorescence in situ hybridization (FISH)

FISH assay was performed to locate circSLC6A6 using a Cy3-labeled probe and to locate miR-1265 using a FAM-labeled probe in HCT8 and RKO cells, respectively. The Cy3-labeled circSLC6A6 probe and FAM-labeled miR-1265 probe were designed and synthesized by GenePharma (Shanghai, China). Cells were seeded in 35-mm glass bottom dishes with 10-mm microwells. After washing with PBS and being fixed with anhydrous ethanol, the cells were treated with 100μl of 0.1% Triton-100 at room temperature for 15 min. The cells were hybridized with 5μl of probe in hybridization buffer (10% dextran sulfate, 40% formamide, 4×saline-sodium citrate (SSC), 1×Denhardt's solution, 1000 mg/ml sheared salmon sperm DNA, 10 mM DDT, 1000 mg/ml yeast transfer RNA) at 37°C overnight. Then, cells were continuously washed and dyed with 100μl of DAPI for 20 min. Then, confocal laser scanning microscopy was used to observe the staining. Simultaneously, FISH assay was also performed in TMA, which contained 106 paired CRC samples by Cy3-labeled miR-1265 (Boster, Shanghai). The staining scores were evaluated by two independent pathologists to avoid bias as previously described in our published study [24]. Finally,

the samples scores were divided into two groups: the high expression group (4-8) and the low expression group (0-3). The sequences of circSLC6A6 and miR-1265 probe for FISH and TMA were listed in Additional file 1: TableS3.

Protein half-life detection

HCT116 p53+/+ cells were respectively stably transfected with shC2CD4A-1, shC2CD4A-2 and pLVX-C2CD4A, and were treated with 10 mg/mL cycloheximide (CHX). Then, the treated cells were harvested after CHX treatment for 0, 20, 40, 60, 90 and 120 min, respectively. Equal amount of protein was extracted from the treated cells which was performed western blotting analysis with anti-C2CD4A or anti-P53 antibody. GAPDH was selected as an internal control to verify basal level expression in different groups.

Immunoprecipitation and Mass Spectrometry (IP/MS)

293T cells transfected with Flag-C2CD4A were lysed in RIPA buffer (20 mM Tris-HCl (pH 8), 137 mM NaCl, 0.5% Triton X-100, 2 mM EDTA) and protease inhibitor cocktail (Sangon Biotech, Shanghai, China). Cell lysates were incubated with Flag-M2 agarose beads (Sigma) overnight and eluted by Flag peptides (Sigma). The Flag peptide elution was resolved on SDS-PAGE and Coomassie blue stained. Lysates from 293T cells transfected with control Flag-vector were served as control. Protein bands specific to the Flag-C2CD4A transfection were digested with trypsin and analyzed by mass spectrometry for protein identification.

Co-immunoprecipitation assay (Co-IP) and ubiquitination assay

Protein extracts were immunoprecipitated with Protein A+G Agarose beads (Beyotime Biotechnology, Shanghai, China) using appropriate antibodies or control IgG (Sigma, USA). Then, the protein of immunocomplexes were subject to immunoblotting analysis with antibodies as indicated. For ubiquitination assay, 293T cells were co-transfected with Flag-C2CD4A, HA-P53 and His-ubiquitin. Alternatively, 293T cells were co-transfected with sh-C2CD4A, HA-P53 and His-ubiquitin. 24 hour later, 293T cells were treated with MG132 (10μM) for 8 hours to inhibit proteasomal degradation. The transfected cells were lysed in lysis buffer. The cell lysates were centrifuged. Then the supernatants were pulled-down by incubation with Ni-NTA beads, and the protein of immunocomplexes was immunoblotted using anti-HA antibody.

RNA immunoprecipitation (RIP)

RIP was performed by using Magna RIP™ RNA-binding protein immunoprecipitation kit (Millipore, Billerica, MA) according to manufacturer's protocol. The AGO2-RIP experiments were conducted in RKO cells transiently overexpressing miR-1265 mimics or miR-NC. 48h later, approximately 1×10^7 RKO cells were lysed in complete RNA lysis buffer. Then, RKO cell lysates were incubated with RIP immunoprecipitation buffer containing magnetic beads conjugated with human anti-Argonaute2 (AGO2) antibody (Millipore, Billerica, MA, USA) or negative control IgG (Millipore, Billerica, MA, USA) at 4℃

overnight. Each sample was digested with Proteinase K and then immunoprecipitated RNA were analyzed by qRT-PCR to test the concentration of circSLC6A6. RIP assay was repeated in triplicate.

RNA Pull-down assay

The biotinylated circSLC6A6 probe and miR-1265 probe were designed and synthesized by GenePharma (Shanghai, China) and the sequences were listed in Additional file 1: TableS4. Briefly, cells were collected, lysed, and sonicated. Probe-coated beads were generated by coincubating the circSLC6A6 and miR-1265 probes with probes-M280 streptavidin dynabeads (Invitrogen, USA) at 25°C for 2h. The cell lysates were incubated with circSLC6A6 and miR-1265 probes or oligo probe at 4°C overnight. After washing with wash buffer, the RNA complexes bound to the beads were eluted and extracted with the RNAisoPlus (TaKaRa, Japan) and measured by qRT-PCR.

Statistical analysis

All quantitative data were enumerated by a $\chi 2$ or Fisher's exact test. The associations were analyzed by Pearson's test. Comparisons between different groups were analyzed using a paired or unpaired t-test. Survival curves were drawn by Kaplan-Meier method and analyzed by log-rank test. The SPSS 23.0 software was deployed for statistical analysis. $P<0.05$ was considered statistically significant in all tests.

Results

C2CD4A is frequently upregulated in CRC

In TCGA database, the volcano plots showed differentially expressed genes in 50 paired CRC samples (41 paired colon cancer and 9 paired rectum cancer) (Fig. 1A). We found that C2CD4A expression was significantly higher in CRC tissues compared with normal tissues (Fig. 1B). C2CD4A was higher in CRC tissues than in normal tissues according to the public GEPIA dataset (Fig. 1C). On the basis of Oncomine database (www.oncomine.org), C2CD4A was also significantly higher in 45 colorectal adenocarcinoma and 36 colorectal carcinoma compared with normal tissues (Skrzypczak Colorectal Statistics, 2010), respectively (Fig. 1D). To further confirm the variation of the expression of C2CD4A in CRC tissues, qRT-PCR indicated upregulation of C2CD4A in 63 pairs of fresh frozen CRC tissues compared to adjacent noncancer tissues (Fig. 1E). Western blotting analysis further confirmed that C2CD4A was upregulated in randomly selected 12 pairs of fresh frozen CRC tissues compared to adjacent noncancer tissues (Fig. 1F). Meanwhile, C2CD4A mRNA and protein expression were also detected in eight CRC cell lines. C2CD4A was presented with the highest expression in RKO cell and with the lowest expression in HCT8 cell respectively (Fig. 1G). Therefore, we chosen RKO and HCT8 cells for subsequent functional assays.

C2CD4A promoted CRC cell growth in vitro and in vivo

To explore the biological functions of C2CD4A in CRC, knockdown and overexpression vectors (sh-Ctrl, sh-C2CD4A-1, sh-C2CD4A-2 and pLVX-Ctrl, pLVX-C2CD4A) were transfected with lentiviral vectors to generate stable knockdown or overexpression cell lines, respectively. The effects of knockdown and

overexpression on C2CD4A expression were confirmed by qRT-PCR and western blotting analysis (Fig. 2A). Subsequently, CCK-8 assay, EdU assay and clone assay results revealed that the growth rate of RKO cell was noticeably attenuated in the downregulated C2CD4A expression groups (Fig. 2B, C and D). However, the growth rate of HCT8 cell was significantly enhanced in the upregulated C2CD4A expression groups (Fig. 2B, C and D). Next, flow cytometry indicated that downregulated expression of C2CD4A increased the percentage of apoptotic RKO cells, whereas upregulated expression of C2CD4A decreased the percentage of apoptotic HCT8 cells (Fig. 2E). Based on in *vitr*o findings, we next tested the role of C2CD4A in *vivo*. A xenograft model was constructed by subcutaneous injection of tumor cells in nude mice. As shown in Fig. 3, the tumor volumes were significantly diminished in knockdown groups (sh-C2CD4A-1, sh-C2CD4A-2 *vs* sh-Ctrl) (Fig. 3B) as monitored once a week. Furthermore, the mean tumor weights of the knockdown groups (sh-C2CD4A-1, sh-C2CD4A-2) were significantly lower than those of the control groups (sh-Ctrl) (Fig. 3C). We then extracted the total RNA and protein from the tumors in different groups. qRT-PCR and western blotting confirmed that the expression of C2CD4A were significantly decreased in knockdown groups (Fig. 3D). Subsequently, western blotting and IHC staining showed that the levels of Ki-67 were obviously decreased by C2CD4A knockdown, while the levels of Cleaved-caspase3 were markedly elevated (Fig. 3D and E). To summarized, these data demonstrated that C2CD4A served as an oncogene in CRC and thus promoted CRC growth both in *vitro* and in *vivo*.

C2CD4A promotes CRC cells growth via P53 signaling pathway

Considering our finding that C2CD4A was related to growth, and apoptosis of CRC cells, we aimed to investigate C2CD4A-relevant molecular mechanism in the process of CRC. The critical role of C2CD4A in CRC motivated us to discover the downstream targets genes that were regulated by C2CD4A. We analyzed the correlation between C2CD4A and other genes in CRC using a cDNA array to identify differentially expressed genes (DEGs) between three pairs knockdown and control cells (RKO/sh-C2CD4A-1 and RKO/sh-Ctrl). According to the results of analysis of DEGs regulated by C2CD4A, 232 and 185 genes were upregulated and downregulated (|fold changes|>1.5, $P < 0.05$), respectively (Fig. 4A), with CDKN1A (P21), BAX, FAS and SESN1 exhibiting the highest expression levels and BCL2, Ki67 and TiGAR exhibiting the lowest expression levels (Additional file 2: TableS5). P21, BAX, FAS, SESN1, TiGAR, and PUMA are all the down-stream genes of P53 transcriptional targets [26, 27]. KEGG pathway analysis of these DEGs revealed that P53 signaling pathway was significantly enriched among the top 10 enrichment-regulated pathways (Fig. 4B). Moreover, we next performed the IP/MS to identify key factors associated with C2CD4A. 293T cells transfected with Flag-C2CD4A was immunoprecipitated by Flag-M2 agarose beads and the interacting proteins were visualized by Coomassie blue staining after electrophoresis and identified by mass spectrometry (Fig. 4C). We found that one interacting protein turned out to be P53 among the Flag-C2CD4A-interacted proteins associated with cell apoptotic (Fig. 4D). As the P53 signaling pathway was of significant influence in the regulation of tumor progression [28], it was inferred that C2CD4A might promote the CRC growth and proliferation by repressing the P53 signaling pathway based on our preliminary results. Thus, we further analyzed the correlation between the expression of C2CD4A and p53 down-stream genes. To verify this hypothesis, we measured the

expression variation of p53 down-stream genes in RKO, HCT116 $p53^{+/+}$ and HCT116 $p53^{-/-}$ cells with stable C2CD4A knockdown. The qRT-PCR results showed that C2CD4A knockdown increased P21, BAX, FAS and SESN1 expressions, and decreased TiGAR expression, while the level of P53 mRNA expression remained the same in RKO and HCT116 $p53^{+/+}$ cells (Fig. 4E, Additional file 3: Fig. S1A). Consistently, western blotting results showed that C2CD4A knockdown had increased the expressions of P21, BAX, and P53 level in HCT116 $p53^{+/+}$ cells (Fig. 4F). But there is no change in HCT116 $p53^{-/-}$ cells (Fig. 4E, F). Moreover, in the CRC xenograft mice model, P53, P21 and BAX protein level were detected by western blotting and IHC. The expression of P53, P21 and Bax were significantly elevated in tumors with RKO/sh-C2CD4A (Fig. 3D, E). More impotantly, the knockdown of C2CD4A obviously diminished the expression of p53 protein (Fig. 3E, F). Together, these data suggested C2CD4A might promote the CRC growth and proliferation by repressing the P53 signaling pathway.

C2CD4A interacts with P53

Since C2CD4A was associated with the growth and proliferation of CRC cells, we focused on C2CD4A regulating P53 and its molecular mechanism according to the results of cDNA array and IP/MS. To address whether C2CD4A interacts with P53, 293T cells were co-transfected with Flag-C2CD4A and HA-P53 at various concentrations, and then P53 expression was detected. P53 expression decreased with incremental dose of C2CD4A, showing a dose-dependent manner between C2CD4A and P53 (Fig. 4G). Doxorubicin (DOX) is a DNA damaging agent that has been conformed to increase P53 expression [29]. To further analyze the relationship between C2CD4A and P53 expression, we used different concentrations of DOX to induce P53 expression, and then observed variations of C2CD4A expression in HCT116 cells. The level of P53 expression gradually elevated with the increasing concentration of DOX, whereas the level of C2CD4A expression gradually decreased (Fig. 4H). Therefore, it manifested a significantly concentration-dependent manner between C2CD4A and P53 expression. In summary, our results indicated that C2CD4A and P53 expression were negatively correlated in a dose-dependent manner.

The former results exhibited that C2CD4A was negatively correlated with the protein level of P53, instead of the mRNA level, indicating P53 might be regulated by C2CD4A at the post-transcriptional level. First, we carried out endogenous immunoprecipitation assay to confirm whether C2CD4A interacted with P53. RKO cells were transfected with Flag-C2CD4A to immunoprecipitate P53 and Flag-C2CD4A, and then anti-P53 and anti-Flag were detected in the immunoprecipitated complexes (Fig. 4I). Next, to further detect the interaction of C2CD4A and P53, exogenous Flag-C2CD4A and HA-P53 were co-transfected into 293T cells, and then Flag-C2CD4A or HA-P53 were respectively immunoprecipitated (Fig. 4L). On the whole, the results demonstrated that exogenous C2CD4A and P53 could also be co-immunoprecipitated mutually. The above results demonstrate that C2CD4A could interact with P53.

C2CD4A decreased half-life of P53 and promoted ubiquitin degradation of P53

The above results demonstrated that C2CD4A could bind with P53 and decrease P53 protein expression. It was speculated that C2CD4A had affected the proteolysis of p53. HCT116 p53+/+ cells with stable

C2CD4A knockdown were treated with MG132, a specific proteasome inhibitor. Then, the results form western blotting analysis indicated that the increased P53 protein expression caused by C2CD4A knockdown were mainly rescued by MG132 (Fig. 5A). In addition, 293T cells, with stable overexpressed C2CD4A, were also treated with proteasome inhibitor MG132. Next, the results from western blotting analysis showed that the decreased expression of P53 caused by C2CD4A overexpression were partially reversed by the treatment of MG132 (Fig. 5A). Above results indicated that C2CD4A medicated the downregulation of P53 by proteasomal degradation. Then, HCT116 p53+/+ cells with stable C2CD4A knockdown were treated with CHX. The results from time-dependent protein degradation rate assays showed that the knockdown of C2CD4A in HCT116 $p53^{+/+}$ cells significantly decreased the P53 degradation rate, and extended the half-life of endogenous p53 protein (Fig. 5B). In contrast, HCT116 $p53^{+/+}$ cells with stable C2CD4A overexpression shortened the half-life of endogenous p53 protein (Fig. 5C). The results indicated that C2CD4A was relevant to stability of P53 protein. Ubiquitin-proteasome was a highly effective protein degradation pathway in eukaryotic cells [30]. It was widely acknowledged that ubiquitin-mediated degradation through the proteasomal pathway was canonical mechanism for regulating P53 protein homeostasis [31]. Moreover, it was discussed that whether C2CD4A was of influence on P53 ubiquitination. Accordingly, Flag-C2CD4A, HA-P53 and His-Ub were co-transfected into 293T cells, which results showed that P53 poly-ubiquitination was elevated in 293T cells (Fig. 5D). Conversely, HA-p53, His-Ub, sh-C2CD4A-1 and sh-C2CD4A-2 were respectively transfected into 293T cells. Downregulated C2CD4A expression significantly inhibited P53 poly-ubiquitination (Fig. 5D). Collectively, this results reveal that C2CD4A increased P53 poly-ubiquitination and thereby promoted its proteasomal degradation.

C2CD4A downregulates expressions of P53 by enhancing the MDM2-P53 interaction

E3 ubiquitin ligase murine double minute (MDM2) was not only a transcriptional target of P53 but also the most important negative mediator for P53 protein stability by binding and ubiquitinating P53 via proteasomal degradation pathway [32, 33]. To confirm MDM2's role in stimulating C2CD4A's down-regulating P53, P53 protein expression level was monitored after that 293T cells were transfected with HA-P53, GFP-MDM2 and Flag-C2CD4A, as determined by immunoprecipitation. Intriguingly, GFP-MDM2 binding to HA-P53 was remarkably elevated in the 293T cells with Flag-C2CD4A transfection (Fig. 5E). Concomitantly, Co-IP assay was performed to figure out the interaction among endogenous P53 and GFP-MDM2 in Flag-C2CD4A-overexpressing HCT116 cells. Much more GFP-MDM2 was bound to endogenous P53 when HCT116 cells were transfected with Flag-C2CD4A (Fig. 5E). To further confirm whether C2CD4A mediates p53 reduction through MDM2, 293T cells, with stable overexpressed C2CD4A, were transfected with siRNAs targeting MDM2 to detect the expression of p53. The results of western blotting showed that C2CD4A decreased the expression of p53, but the expression of p53 was not obviously decreased when the silencing of MDM2 (Fig. 5F). Thus, this data strongly suggested that MDM2 was necessary in the interaction process of p53 and C2CD4A, and MDM2 was vital in C2CD4A's negatively regulating P53.

MiR-1265 was downregulated in CRC and suppressed C2CD4A expression by directly binding to the 3'UTR of C2CD4A mRNA

Accumulating evidences indicated that altered expressions of miRNAs were involved in tumor cell proliferation, apoptosis, metabolism, and metastasis [34]. Based on our previous studies on miRNAs in gastrointestinal tumors [19, 24, 25, 35], it was aimed to further figure out whether the overexpression of C2CD4A in CRC was caused by a specific miRNAs dysregulation. Using bioinformatics databases, such as Targetscan, miRWalk and Microrna.org, among those miRNAs which could bind with 3'UTR of C2CD4A, we preliminarily screened out hsa-miR-339-3p, hsa-miR-3153, hsa-miR-361-5p, hsa-miR-3186-5p, hsa-miR-764, hsa-miR-556-3p, hsa-miR-1265, hsa-miR-4290 and hsa-miR-3159 as potential regulators of C2CD4A (Fig. 6A). For above potential regulators, it was found that hsa-miR-339-3p, hsa-miR-361-5p and miR-1265 had been reported in different tumors [36–39], in which hsa-miR-339-3p and hsa-miR-361-5p were lowly expressed in CRC and had assumed the role of tumor suppressing [40, 41]. Next, we used qRT-PCR to detect the expression of miR-339-3p, hsa-miR-361-5p and miR-1265 in 63 pairs fresh frozen CRC tissues, and found that miR-1265 was significant lower in 63 pairs fresh frozen CRC tissues (48/63, 76.2%) compared with those adjacent noncancer tissues (Fig. 6B, Additional file 4: Fig. S2A). Next, according to Pearson's analysis, the qRT-PCR results indicated that miR-1265 expression was significantly lower in CRC tissues than in paired normal tissues and was negatively correlated with C2CD4A mRNA expression in the above CRC samples (r=-0.347, P = 0.005) (Additional file 4: Fig. S2B). However, C2CD4A expression was not significantly correlated with miR-339-3p and miR-361-5p expression (Additional file 4: Fig. S2B). Hence it was speculated that miR-1265 might be the upstream miRNA that regulate C2CD4A expression. Based on current studies, it was shown that miR-1265 served as a tumor suppressor in bladder cancer, glioma, and osteosarcoma [36, 37, 42]. Then, the results of FISH assay using TMA showed that miR-1265 was significantly downregulated in 106 pairs of CRC tissues compared with paired adjacent noncancer tissues (Fig. 6C). However, there was no obvious relationship between miR-1265 expression and different clinicopathological features (Additional file 5: Table S6), including the prognosis of CRC patients (data not shown). To explore whether miR-1265 inhibited the endogenous expression of C2CD4A, miR-1265/mimics and miR-1265/inhibitor were constructed. qRT-PCR and western blotting analysis indicated that C2CD4A mRNA and protein expression was significantly downregulated in the miR-1265/mimics. However, miR-1265/inhibitor induced the opposite experimental results (Fig. 6D, E). It was forecasted by the databases of Targetscan and Microrna.org that there were two binding sites connected by miR-1265 and 3'UTR of C2CD4A. Then, the 3'UTR of C2CD4A, which was predicted to interact with miR-1265, was cloned into a luciferase reporter vector (wild type, WT). Additionally, a reporter carrying two mutated miR-1265 binding sites was also created (Mutant) (Fig. 6F). Luciferase results indicated that inhibited luciferase activity in the cell lysates had transfected with miR-1265/mimics comparing to those transfected with the negative control mimics in the 293T and RKO cells, and were of no effect on the RKO cells with Mutant vectors (Fig. 6G). On the contrary, the luciferase activity in the cell lysates transfected with miR-1265/inhibitor was increased in the HCT8 cells, compared with those transfected with the negative control inhibitor, but did not strengthen luciferase activity in those with Mutant vectors (Fig. 6G). The aforementioned consequences indicated that miR-1265 directly targeted the 3'UTR of C2CD4A mRNA and suppressed C2CD4A mRNA translation in CRC.

MiR-1265 inhibits cell growth, proliferation, and promotes apoptosis in vitro

To explore the possible underlying biological mechanism of miR-1265 function in CRC cells, the results from cell counting assays which included CCK-8 assays, clone formation assays and EdU assays demonstrated that miR-1265/mimics significantly inhibited the growth and proliferation of RKO cells (Additional file 6: Fig. S3A, B and C), while miR-1265/inhibitor promoted growth and proliferation of HCT8 cells (Additional file 5: Fig. S3A, B and C). Meanwhile, miR-1265/mimics increased the proportion of apoptosis cells in RKO (Additional file 6: Fig. S3D), while miR-1265/inhibitor decreased apoptosis cells in HCT8 (Additional file 6: Fig. S3D). In conclusion, miR-1265 had inhibited cell growth, proliferation and promoted cell apoptosis in CRC.

CircSLC6A6 is upregulated in CRC tissues and correlates with the poor prognosis of CRC patients

Extensive evidences confirmed that circRNAs was of great significance in tumor progression [43]. To identify the underlying dysregulated circRNAs in the CRC, RNA-seq analyses was performed to detect differentially expressed circRNAs between in 12 paired fresh frozen CRC tissues and corresponding adjacent normal colorectal mucosae tissues. We found that 373 differentially expressed circRNAs were identified with fold changes > 2 or < 0.5 ($P < 0.05$) (Fig. 7A). Differentially expressed circRNAs which included hsa_circ_0023984, hsa_circ_0008192, hsa_circ_0008694, hsa_circ_0004705 and hsa_circ_0001153 were highly expressed in CRC. Combined with CircInteractome database (https://circinteractome.nia.nih.gov/), bioinformatics analysis revealed that hsa_circ_0004705, which also named circSLC6A6, had possessed miR-1265 binding sites (Fig. 8D) and was significantly upregulated in CRC comparing to the normal colorectal (Additional file 7: Fig. S4A, B). Therefore, we focused on circSLC6A6, which was spliced from the SLC6A6 gene on chr3: 3p21: 45,695,388 – 45,699,581, with an ultimate length of 610 nucleotides. By comparing SLC6A6 mRNA sequences with the expected sequences of circSLC6A6 acquired from circBase (http://www.circbase.org/), schematic diagram illustrated that circSLC6A6 was originated from exons 3, 4 and 5 of its parental SLC6A6 pre-mRNA (Fig. 7B). It was further confirmed the splicing sites via Sanger sequencing (Fig. 7B). However, head-to-tail splicing could be the result of not only trans-splicing but also genomic rearrangements [44]. To mark off above two varieties, special divergent primers to amplify circSLC6A6 and convergent primers for circSLC6A6 mRNA were designed. cDNA and gDNA were extracted separately from RKO and HCT8 cells which were subjected to nucleic acid electrophoresis detection. It was indicated that hat circSLC6A6 could be detected only in cDNA, with no products were detected in the extracted gDNA (Fig. 7C). Being able to resist the digestion by RNase R exonuclease further confirmed that this RNA was in the form of ring. As shown in Fig. 7D, the expression level of linear SLC6A6 obviously dropped after the treatment of RNase R, meanwhile, RNase R was incapable of digesting circSLC6A6. Furthermore, the results of nuclear cytoplasmic fractionation illustrated that circSLC6A6 was mainly positioned in the cytoplasm (Fig. 7E). Next, circSLC6A6 was prominently expressed in CRC cell lines in comparation with FHC cell line via qRT-PCR. Among CRC cell lines, RKO showed the highest level of circSLC6A6, whereas HCT8 the lowest level (Fig. 7F). Additionally, the FISH results also showed that circSLC6A6 was mainly located in cytoplasm (Fig. 7G). All these results confirmed that circSLC6A6 was highly stable in cytoplasm of CRC cells. Then, qRT-PCR assays indicated circSLC6A6 were significantly overexpressed in 63 pairs (49/63, 77.8%) fresh frozen CRC tissues compared to adjacent noncancer tissues (Additional file 7: Fig. S4A, B). More

importantly, compared with colorectal cancer patients with lower circSLC6A6 expression (n = 31), the patients with higher circSLC6A6 expression (n = 32) has a relatively poor OS (P = 0.031) and DFS (P = 0.007) survival (Fig. 7I). All those findings suggested that circSLC6A6 was upregulated both in CRC cells and tissues and was a vital role in diagnosis and prognosis of CRC.

CircSLC6A6 functions as an efficient miR-1265 sponge, and alters the expression of C2CD4A and P53 through miR-1265

Numerous studies have reported that circRNAs might function as miRNA sponges to abrogate the functions of miRNAs [44, 45]. Hence, we explored whether circSLC6A6 promoted CRC growth and proliferation by sponging miRNAs. Firstly, by utilizing CircInteractome database, it was predicted that the potential target miRNAs of circSLC6A6 and the possible downstream miRNAs. It was indicted that miR-1265 shared binding site with circSLC6A6 attracted our attention. The FISH results revealed that co-location of circSLC6A6 and miR-1265 were mainly located in cytoplasm (Fig. 8A). In addition, overexpressed circSLC6A6 was negatively correlated with miR-1265 expression (r=-0.482, P < 0.0001) in 63 paired CRC tissues and adjacent noncancer tissues, and positively associated with C2CD4A expression(r = 0.369, P = 0.003) (Fig. 8B), which indicated that circSLC6A6 might be involved in regulating miR-1265 and C2CD4A expression. All the results revealed that circSLC6A6 might interact with miR-1265 in CRC. To address the regulation of circSLC6A6 on miR-1265, three circSLC6A6-targeting siRNAs (si-circ-1, si-circ-2, si-circ-3) and a circSLC6A6 overexpression vector (pEX3-circ) were constructed to alter the expression of circSLC6A6. The result of qRT-PCR showed that the altered expression of circSLC6A6 had no significantly effect on the expression of SLC6A6 mRNA (Additional file 7: Fig. S4C, D). Then, we monitored the effect of altered circSLC6A6 expression on miR-1265 expression. Downregulation of circSLC6A6 could decrease miR-1265 expression and upregulation one could increase miR-1265 expression in RKO and HCT8 cells, respectively (Fig. 8C). Additionally, full length circSLC6A6 sequences (WT, wild type) and sequences with mutant binding site (Mutant) were constructed (Fig. 8D). Luciferase reporter assay results indicated that miR-1265/inhibitor relatively strengthened the luciferase activity of vector containing wild circSLC6A6 but did not alter the luciferase activity of the vector containing mutant circSLC6A6 (Fig. 8E). Conversely, miR-1265/mimics relatively subdued the luciferase activity of vector with wild circSLC6A6 but did not decrease the vector with mutant circSLC6A6 (Fig. 8E).

Next, RIP assays using anti-AGO2 or IgG were carried out in RKO cells with transiently transfected with miR-1265 mimics or controls, followed by agarose gel electrophoresis qRT-PCR and analysis for circSLC6A6 levels (Fig. 8F). The RIP results showed that circSLC6A6 pulled down with anti-AGO2 antibody was significantly enriched in RKO cells after being transfected with miR-1265 mimics compared to controls, suggesting that miR-1265 could directly target circSLC6A6 in AGO2 manner. Moerover, RNA pull-down assay indicated that endogenous miR-1265 or circSLC6A6 were significantly pulled down by biotinylated probes against miR-1265 or circSLC6A6, displaying the existence of circSLC6A6/miR-1265 complexes. The results indicated that specific overexpression miR-1265 was detected in the circSLC6A6 pull-down pellet. Moreover, more circSLC6A6 was captured in the biotin-miR-1265 groups than in the biotin-negative control (NC) groups (Fig. 8G), suggesting that circSLC6A6 served as an effient miR-1265

sponge. Moreover, downregulation of circSLC6A6 markedly attenuated the expression of C2CD4A and MDM2, and increased the expression of P53, P21, Bax, and MDM2 (Additional file 7: Fig. S4E). Conversely, upregulation of circSLC6A6 enhanced the expression of C2CD4A and MDM2, and decreased the expression of P53, P21, Bax, and MDM2, which indicated that circSLC6A6 positively regulated the expression of C2CD4A (Additional file 7: Fig. S4F). However, miR-1265/inhibitor partly reversed the decreased expression C2CD4A induced by downregulated circSLC6A6 expression, and miR-1265/mimics reversed the overexpression of C2CD4A induced by upregulated circSLC6A6 expression, indicating that miR-1265 could reverse the regulation of circSLC6A6 on C2CD4A expression (Additional file 7: Fig. S4E, F). Therefore, we demonstrated that circSLC6A6 acted as miR-1265 sponge and lessen the repressive effect of miR-1265 on C2CD4A and P53 expression, thereby upregulating C2CD4A and downregulating P53 expression. Collectively, these results unveiled a new mechanism that circSLC6A6 acted as a miR-1265 sponge to promote the proliferation of CRC through enhancing C2CD4A expression.

CircSLC6A6 promotes cell growth, proliferation, and inhibits apoptosis in vitro

To assess the biological function of circSLC6A6 in CRC cells, RKO cells with high circSLC6A6 expression and HCT8 cells with low circSLC6A6 expression were chosen to explore the function of underlying biological mechanism of circSLC6A6 in CRC (Fig. 7F). The results from cell counting assays which included CCK-8 assays, EdU assays and clone formation assays demonstrated that downregulated circSLC6A6 significantly inhibited the growth and proliferation of RKO cells (Additional file 8: Fig. S5A, B and C), while the upregulated circSLC6A6 remarkably promoted the growth and proliferation of HCT8 cells (Additional file 8: Fig. S5A, B and C). Meanwhile, downregulated circSLC6A6 increased the rate of apoptosis cells in RKO (Additional file 8: Fig. S5D), while upregulated circSLC6A6 decreased the rate of HCT8 apoptosis cells (Additional file 8: Fig. S5D). Collectively, these data confirmed that circSLC6A6 promoted cell growth, proliferation and inhibited cell apoptosis in CRC.

Discussion

In our present results, we firstly revealed that C2CD4A was significantly upregulated in CRC tissues and cells. To clarify the role of C2CD4A in CRC, it was observed that C2CD4A integrated with P53 to promote ubiquitin degradation of P53 through increasing interaction of MDM2 with P53. Additionally, our results showed that circSLC6A6 regulated C2CD4A and P53 expression by sponging miR-1265 to promote growth of CRC cells. Above findings was the first to explore the function of circSLC6A6/miR-1265/C2CD4A/P53 axis in the growth of CRC.

C2CD4A, which usually conferring human diabetes susceptibility was firstly reported as a gene relevant to CRC in our study related to CRC. It was found that the knockdown or overexpression of C2CD4A was capable of inhibiting or facilitating the growth of CRC cell via CCK-8, colony formation and EdU assays, which was also verified in *vivo* tumor xenograft assays. Consistently, knockdown or overexpression of C2CD4A markedly promoted or repressed cell apoptosis in *vitro*. Our findings therefore showed that C2CD4A served as an oncogene could promote CRC growth, and inhibited cell apoptosis. To further reveal

the roles of C2CD4A in CRC, our attention was focused on the downstream molecular mechanisms underlying C2CD4A. The expression of C2CD4A in RKO cells was knocked-down, and cDNA arrays were performed to screen for altered genes. According to the results of analysis of DEGs and KEGG analysis, we speculated that C2CD4A might promote the CRC growth and proliferation by repressing the P53 signaling pathway. IP/MS also confirmed that C2CD4A may interact with P53. It was being well acknowledged that ubiquitination-induced proteasomal degradation of P53 was essential to maintain P53 protein homeostasis [46, 47], whose disruption was a molecular marker for cancer in recent 40 years. It was demonstrated by Wang et al. that TRIM67, a transcriptional target of P53, functioned as a tumor suppressor by directly binding with the C terminus of P53 and protecting it from MDM2-mediated ubiquitination in CRC [48]. Yet, the regulation aberrant expression of P53 protein had not been thoroughly studied [49]. In this study, we firstly described the aberrant upregulated C2CD4A in CRC tissue and its critical role in regulating P53 protein stability, C2CD4A regulated the expression of P53 target genes, including P21 and BAX. We also found that C2CD4A shortened half-life of P53, suggesting that C2CD4A might promote CRC oncogenesis through decreasing P53 function. Furthermore, P53 accumulation was enhanced in C2CD4A-silenced HCT116 p53+/+ cells. Next, we confirmed that C2CD4A, as a novel regulator of the P53 pathway, interacted with P53 and promoted P53 ubiquitination and degradation. Thus, C2CD4A-mediated P53 degradation implied that C2CD4A might be critical for CRC growth and tumorigenesis. The E3 ubiquitin ligase MDM2 had acted as a vital negative regulator of P53 protein level and activity among plenty of proteins which involved in P53 regulation [32]. MDM2 was bound to P53 and ubiquitinates it proteasomal degradation. Intriguingly, the upregulated C2CD4A expression was able to increase the binding of MDM2 and P53 to facilitate P53 degradation. These results indicated that C2CD4A mediated P53 ubiquitin-degradation through increasing the interaction of MDM2 with P53. MDM2 might be a vital factor in C2CD4A mediated-P53 ubiquitination.

Numerous studies shown that aberrantly expressed miRNAs had regulated CRC development and progression [22, 50]. Currently, the biological function of miR-1265 served as a tumor-suppressive role in several cancers and its molecular targets in the process of tumorigenesis had been illustrated in several studies [36, 37, 42]. In this research, we found that miR-1265 was significantly downregulated in CRC tissues and cell lines for the first time. Subsequently, our research demonstrated that miR-1265 was directly bound to 3’UTR of C2CD4A to restrain C2CD4A protein expression and therefore inhibited the progress of CRC, which was also verified through a series of functional experiments such as CCK-8, colony formation, EdU and apoptosis assays. Luciferase reporter assay also verified that miR-1265 directly targeting C2CD4A in CRC cells. Taken together, our results demonstrated, for the first time, that miR-1265 was a tumor suppressive element by targeting C2CD4A in CRC.

Currently, circRNAs served as the most popular topic in the field of carcinogenesis and cancer progression. Increasing evidences disclosed that circRNAs were involved in the regulation of cancer cell proliferation, survival, migration and differentiation [19, 22, 25, 51]. However, the miRNA sponge is still the most common mechanism by which circRNA functions [19, 52]. In particular, our previous study indicated that circMLLT10 served as a ceRNA, a sponge of miR-509-3-5p, promoted gastric cancer cell growth and metastasis via increasing the expression of GINS4 and then activating Rac1 and CDC42 [25]. Moreover,

our recently study demonstrated that circCCDC9 directly sponged miR-6792-3p to relieve the repressive effect of miR-6792-3p on its target CAV1, and then to suppress the progression of gastric cancer [24]. Circ-ITCH up-regulates p21 and PTEN through sponging miR-17 and miR-224, which suppressed the aggressive biological behaviors of bladder cancer [53]. In this study, it was identified that a novel circRNA-circSLC6A6 derived from SLC6A6 gene, which was highly expressed in CRC tissue and was capable of sponging miR-1265, and thus diminished miR-1265's inhibiting effect on C2CD4A and stimulated CRC growth and proliferation. There were several pieces of evidence implicating that circSLC6A6 functioned as a sponge of miR-1265 to regulate C2CD4A in CRC. First, circSLC6A6 expression negatively correlated with miR-1265, whereas positively correlated with C2CD4A expression in 63 fresh frozen CRC tissues. Second, downregulated circSLC6A6 would separately lead to a lower miR-1265 and higher C2CD4A and up-regulated circSLC6A6 worked the opposite way. Third, bioinformatics analyses and luciferase reporter assays verified this prediction. Fourth, inhibition of miR-1265 reversed the effect of downregulated C2CD4A expression caused by knockdown of circSLC6A6, and overexpression of miR-1265 reversed the effect of upregulated C2CD4A expression caused by overexpression of circSLC6A6. Finally, circSLC6A6 could regulate C2CD4A expression, thus leading to the C2CD4A-reduced P53 degradation and inhibiting downstream pathway (Fig. 8H). In conclusion, circSLC6A6 was demonstrated to be an important candidate oncogene in CRC and was involved in the prognosis of CRC patients. CRC patients with high circSLC6A6 expression had lower OS and DFS. CircSLC6A6 might act as a miR-1265 sponge to abolish the inhibitory effects on C2CD4A expression, which eventually promoted the growth and proliferation of CRC cells. Our study revealed that the circSLC6A6/miR-1265/C2CD4A/P53 axis was involved in the pathogenesis and development of CRC, indicating that this axis might be a novel therapeutic target in patients with CRC.

Conclusion

In summary, our results reveals that circSLC6A6/miR-1265/C2CD4A axis, which was involved in CRC growth via the P53 signaling pathway, may provide a new therapeutic target for CRC.

Abbreviations

AJCC: American Joint Commission on Cancer; CHX: cycloheximide; CircRNA: C2CD4A: C2 calcium dependent domain containing 4A; Circular RNA; ceRNA: Competing endogenous RNA; CRC: Colorectal cancer; DEGs: differentially expressed genes; DFS: Disease-free survival; DOX: Doxorubicin; FISH: Fluorescence in situ hybridization; IHC: Immunohistochemistry; IP/MS: Immunoprecipitation and Mass Spectrometry; miRNA: MicroRNA; KEGG Kyoto Encyclopedia of Genes and Genomes; qRT-PCR: Real-time quantitative polymerase chain reaction; OS: Overall survival; RIP: RNA immunoprecipitation; TMA: Tissue microarray; 3'UTR: 3'-untranslated region; SIX1: Sine oculis homeobox homolog 1. SLC6A6: solute carrier family 6 member 6. TRIM67: tripartite motif containing 67.

Declarations

Acknowledgements

Not applicable.

Ethics approval and consent to participate

This work was ratified by the Ethics Committee of Shanghai General Hospital. All animals were used according to the Shanghai General Hospital Animal Care and Use Guidelines. Written informed consents were obtained from all patients.

Consent for publication

All authors consent for publication.

Availability of data and materials

The data sets used in this study can be obtained from the corresponding author on reasonable request.

Competing interests

The authors declare no conflicts of interest in this article.

Funding

This work was supported by grants from the National Natural Science Foundation of China (81772526 and 82072662) received by C. H., Shanghai Municipal Education Commission-Gaofeng Clinical Medicine Grant Support (20161425) received by C. H., Shanghai Jiaotong University Medical Cross Fund (YG2017MS28) received by C. H., Shanghai.

Authors' contributors

C. H. and ZY. R. designed the experiments and revised the manuscript. ZY. R. performed the main experiments and wrote the manuscript. Z. L., ZM. F., PS. Z., gathered and analyzed the raw data. JM. Z., TF. L., ZL. Z., ZL.Y. Q.L. and ZJ. Q. performed the experiments. All authors provided supervision and approved the manuscript.

References

1. Miller KD, Goding Sauer A, Ortiz AP, Fedewa SA, Pinheiro PS, Tortolero-Luna G, et al. Cancer Statistics for Hispanics/Latinos, 2018. CA Cancer J Clin. 2018;68(6):425-45.
2. O'Connell JB, Maggard MA, Ko CY. Colon cancer survival rates with the new American Joint Committee on Cancer sixth edition staging. J Natl Cancer Inst. 2004;96(19):1420-5.
3. Siegel RL, Miller KD, Jemal A. Cancer statistics, 2016. CA Cancer J Clin. 2016;66(1):7-30.

4. Zhang Y, Chen Z, Li J. The current status of treatment for colorectal cancer in China: A systematic review. Medicine (Baltimore). 2017;96(40):e8242.
5. Jeong SY, Chessin DB, Schrag D, Riedel E, Wong WD, Guillem JG. Re: Colon cancer survival rates with the new American Joint Committee on Cancer sixth edition staging. J Natl Cancer Inst. 2005;97(22):1705-6; author reply 6-7.
6. Xie L, Gao S, Alcaire SM, Aoyagi K, Wang Y, Griffin JK, et al. NLF-1 delivers a sodium leak channel to regulate neuronal excitability and modulate rhythmic locomotion. Neuron. 2013;77(6):1069-82.
7. Kycia I, Wolford BN, Huyghe JR, Fuchsberger C, Vadlamudi S, Kursawe R, et al. A Common Type 2 Diabetes Risk Variant Potentiates Activity of an Evolutionarily Conserved Islet Stretch Enhancer and Increases C2CD4A and C2CD4B Expression. Am J Hum Genet. 2018;102(4):620-35.
8. Kaiser AM, Attardi LD. Deconstructing networks of p53-mediated tumor suppression in vivo. Cell Death Differ. 2018;25(1):93-103.
9. Oren M. Decision making by p53: life, death and cancer. Cell Death Differ. 2003;10(4):431-42.
10. Schulz-Heddergott R, Stark N, Edmunds SJ, Li J, Conradi LC, Bohnenberger H, et al. Therapeutic Ablation of Gain-of-Function Mutant p53 in Colorectal Cancer Inhibits Stat3-Mediated Tumor Growth and Invasion. Cancer Cell. 2018;34(2):298-314.e7.
11. Bahnassy AA, Zekri AR, Salem SE, Abou-Bakr AA, Sakr MA, Abdel-Samiaa AG, et al. Differential expression of p53 family proteins in colorectal adenomas and carcinomas: Prognostic and predictive values. Histol Histopathol. 2014;29(2):207-16.
12. Kubbutat MH, Jones SN, Vousden KH. Regulation of p53 stability by Mdm2. Nature. 1997;387(6630):299-303.
13. Memczak S, Jens M, Elefsinioti A, Torti F, Krueger J, Rybak A, et al. Circular RNAs are a large class of animal RNAs with regulatory potency. Nature. 2013;495(7441):333-8.
14. Su Y, Zhong G, Jiang N, Huang M, Lin T. Circular RNA, a novel marker for cancer determination (Review). Int J Mol Med. 2018;42(4):1786-98.
15. Vo JN, Cieslik M, Zhang Y, Shukla S, Xiao L, Zhang Y, et al. The Landscape of Circular RNA in Cancer. Cell. 2019;176(4):869-81.e13.
16. Pamudurti NR, Bartok O, Jens M, Ashwal-Fluss R, Stottmeister C, Ruhe L, et al. Translation of CircRNAs. Mol Cell. 2017;66(1):9-21.e7.
17. Barrett SP, Salzman J. Circular RNAs: analysis, expression and potential functions. Development. 2016;143(11):1838-47.
18. Karreth FA, Pandolfi PP. ceRNA cross-talk in cancer: when ce-bling rivalries go awry. Cancer Discov. 2013;3(10):1113-21.
19. Zhu Z, Rong Z, Luo Z, Yu Z, Zhang J, Qiu Z, et al. Circular RNA circNHSL1 promotes gastric cancer progression through the miR-1306-3p/SIX1/vimentin axis. Mol Cancer. 2019;18(1):126.
20. Xie F, Li Y, Wang M, Huang C, Tao D, Zheng F, et al. Circular RNA BCRC-3 suppresses bladder cancer proliferation through miR-182-5p/p27 axis. Mol Cancer. 2018;17(1):144.

21. Liang WC, Wong CW, Liang PP, Shi M, Cao Y, Rao ST, et al. Translation of the circular RNA circβ-catenin promotes liver cancer cell growth through activation of the Wnt pathway. Genome Biol. 2019;20(1):84.
22. Jian X, He H, Zhu J, Zhang Q, Zheng Z, Liang X, et al. Hsa_circ_001680 affects the proliferation and migration of CRC and mediates its chemoresistance by regulating BMI1 through miR-340. Mol Cancer. 2020;19(1):20.
23. Rong Z, Luo Z, Zhang J, Li T, Zhu Z, Yu Z, et al. GINS complex subunit 4, a prognostic biomarker and reversely mediated by Kruppel-like factor 4, promotes the growth of colorectal cancer. Cancer Sci. 2020;111(4):1203-17.
24. Luo Z, Rong Z, Zhang J, Zhu Z, Yu Z, Li T, et al. Circular RNA circCCDC9 acts as a miR-6792-3p sponge to suppress the progression of gastric cancer through regulating CAV1 expression. Mol Cancer. 2020;19(1):86.
25. Zhu Z, Yu Z, Rong Z, Luo Z, Zhang J, Qiu Z, et al. The novel GINS4 axis promotes gastric cancer growth and progression by activating Rac1 and CDC42. Theranostics. 2019;9(26):8294-311.
26. Hu W, Chen S, Thorne RF, Wu M. TP53, TP53 Target Genes (DRAM, TIGAR), and Autophagy. Adv Exp Med Biol. 2019;1206:127-49.
27. Cordani M, Butera G, Dando I, Torrens-Mas M, Butturini E, Pacchiana R, et al. Mutant p53 blocks SESN1/AMPK/PGC-1alpha/UCP2 axis increasing mitochondrial O2-. production in cancer cells. Br J Cancer. 2018;119(8):994-1008.
28. Yue X, Zhao Y, Xu Y, Zheng M, Feng Z, Hu W. Mutant p53 in Cancer: Accumulation, Gain-of-Function, and Therapy. J Mol Biol. 2017;429(11):1595-606.
29. Shamseddine AA, Clarke CJ, Carroll B, Airola MV, Mohammed S, Rella A, et al. P53-dependent upregulation of neutral sphingomyelinase-2: role in doxorubicin-induced growth arrest. Cell Death Dis. 2015;6:e1947.
30. Ciechanover A. The ubiquitin-proteasome proteolytic pathway. Cell. 1994;79(1):13-21.
31. Chao CC. Mechanisms of p53 degradation. Clin Chim Acta. 2015;438:139-47.
32. Oliner JD, Pietenpol JA, Thiagalingam S, Gyuris J, Kinzler KW, Vogelstein B. Oncoprotein MDM2 conceals the activation domain of tumour suppressor p53. Nature. 1993;362(6423):857-60.
33. Karni-Schmidt O, Lokshin M, Prives C. The Roles of MDM2 and MDMX in Cancer. Annu Rev Pathol. 2016;11:617-44.
34. Lee YS, Dutta A. MicroRNAs in cancer. Annu Rev Pathol. 2009;4:199-227.
35. Zhang J, Zhu Z, Sheng J, Yu Z, Yao B, Huang K, et al. miR-509-3-5P inhibits the invasion and lymphatic metastasis by targeting PODXL and serves as a novel prognostic indicator for gastric cancer. Oncotarget. 2017;8(21):34867-83.
36. Yan D, Dong W, He Q, Yang M, Huang L, Kong J, et al. Circular RNA circPICALM sponges miR-1265 to inhibit bladder cancer metastasis and influence FAK phosphorylation. EBioMedicine. 2019;48:316-31.

37. Pan G, Hu T, Chen X, Zhang C. Upregulation Of circMMP9 Promotes Osteosarcoma Progression Via Targeting miR-1265/CHI3L1 Axis. Cancer Manag Res. 2019;11:9225-31.
38. Weber CE, Luo C, Hotz-Wagenblatt A, Gardyan A, Kordass T, Holland-Letz T, et al. miR-339-3p Is a Tumor Suppressor in Melanoma. Cancer Res. 2016;76(12):3562-71.
39. Ma F, Zhang L, Ma L, Zhang Y, Zhang J, Guo B. MiR-361-5p inhibits glycolytic metabolism, proliferation and invasion of breast cancer by targeting FGFR1 and MMP-1. J Exp Clin Cancer Res. 2017;36(1):158.
40. Ma F, Song H, Guo B, Zhang Y, Zheng Y, Lin C, et al. MiR-361-5p inhibits colorectal and gastric cancer growth and metastasis by targeting staphylococcal nuclease domain containing-1. Oncotarget. 2015;6(19):17404-16.
41. Zhou C, Lu Y, Li X. miR-339-3p inhibits proliferation and metastasis of colorectal cancer. Oncol Lett. 2015;10(5):2842-8.
42. Gao F, Du Y, Zhang Y, Ren D, Xu J, Chen D. Circ-EZH2 knockdown reverses DDAH1 and CBX3-mediated cell growth and invasion in glioma through miR-1265 sponge activity. Gene. 2020;726:144196.
43. Zhong Y, Du Y, Yang X, Mo Y, Fan C, Xiong F, et al. Circular RNAs function as ceRNAs to regulate and control human cancer progression. Mol Cancer. 2018;17(1):79.
44. Deng G, Mou T, He J, Chen D, Lv D, Liu H, et al. Circular RNA circRHOBTB3 acts as a sponge for miR-654-3p inhibiting gastric cancer growth. J Exp Clin Cancer Res. 2020;39(1):1.
45. Hong X, Liu N, Liang Y, He Q, Yang X, Lei Y, et al. Circular RNA CRIM1 functions as a ceRNA to promote nasopharyngeal carcinoma metastasis and docetaxel chemoresistance through upregulating FOXQ1. Mol Cancer. 2020;19(1):33.
46. Wade M, Li YC, Wahl GM. MDM2, MDMX and p53 in oncogenesis and cancer therapy. Nat Rev Cancer. 2013;13(2):83-96.
47. Huang C, Wu S, Ji H, Yan X, Xie Y, Murai S, et al. Identification of XBP1-u as a novel regulator of the MDM2/p53 axis using an shRNA library. Sci Adv. 2017;3(10):e1701383.
48. Wang S, Zhang Y, Huang J, Wong CC, Zhai J, Li C, et al. TRIM67 Activates p53 to Suppress Colorectal Cancer Initiation and Progression. Cancer Res. 2019;79(16):4086-98.
49. Ni T, Li XY, Lu N, An T, Liu ZP, Fu R, et al. Snail1-dependent p53 repression regulates expansion and activity of tumour-initiating cells in breast cancer. Nat Cell Biol. 2016;18(11):1221-32.
50. Noorolyai S, Baghbani E, Aghebati Maleki L, Baghbanzadeh Kojabad A, Shanehbansdi D, Khaze Shahgoli V, et al. Restoration of miR-193a-5p and miR-146 a-5p Expression Induces G1 Arrest in Colorectal Cancer through Targeting of MDM2/p53. Adv Pharm Bull. 2020;10(1):130-4.
51. Yang H, Li X, Meng Q, Sun H, Wu S, Hu W, et al. CircPTK2 (hsa_circ_0005273) as a novel therapeutic target for metastatic colorectal cancer. Mol Cancer. 2020;19(1):13.
52. Huang WJ, Wang Y, Liu S, Yang J, Guo SX, Wang L, et al. Silencing circular RNA hsa_circ_0000977 suppresses pancreatic ductal adenocarcinoma progression by stimulating miR-874-3p and inhibiting

PLK1 expression. Cancer Lett. 2018;422:70-80.

53. Yang C, Yuan W, Yang X, Li P, Wang J, Han J, et al. Circular RNA circ-ITCH inhibits bladder cancer progression by sponging miR-17/miR-224 and regulating p21, PTEN expression. Mol Cancer. 2018;17(1):19.

Figures

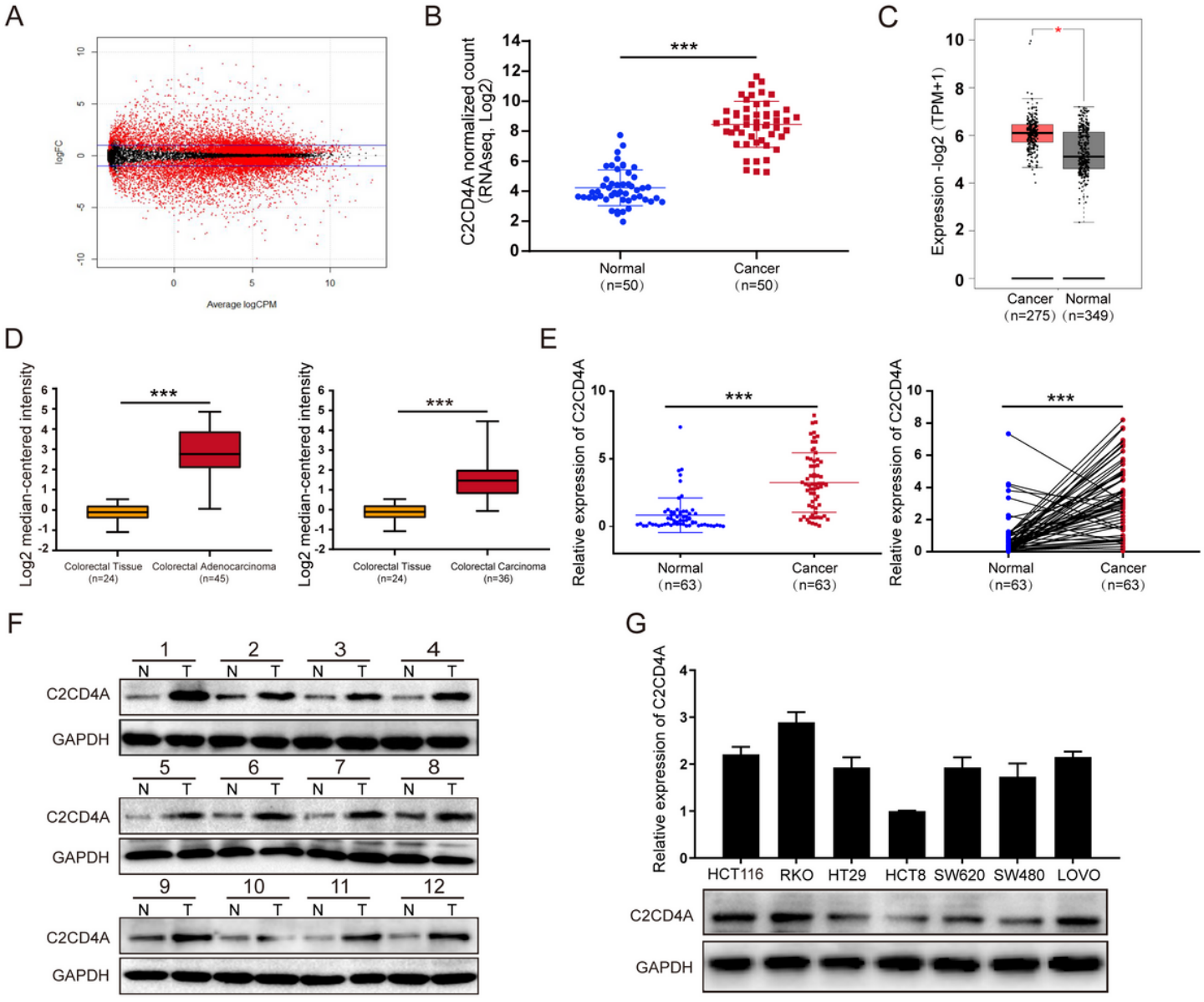

Figure 1

C2CD4A expressions in CRC tissues and cell lines. a The scatter diagram showed the differential mRNA expression among 50 CRC cancer samples and paired adjacent normal colorectal mucosae samples from TCGA database. b Relative C2CD4A mRNA expression in 50 paired CRC tissues and paired adjacent normal colorectal mucosae from TCGA database. c The expression of C2CD4A was significantly higher in

CRC tissues than in normal tissues in the GEPIA dataset. Mean and SD are presented (num (Normal) = 349, num (Cancer) = 275, P < 0.05 as calculated by t-test). d C2CD4A expression in CRC specimens from the Oncomine datasets (Skrzypczak Colorectal Statistics, 2010). e C2CD4A expression was elevated in 63 fresh frozen CRC tissues samples compared with paired adjacent normal mucosae by using qRT-PCR. f C2CD4A protein expressions in representative paired CRC tissue samples were detected by western blotting. g qRT-PCR and western blotting helped to detect the expression of C2CD4A in 7 CRC cell lines. (**P <0.01, ***P <0.001).

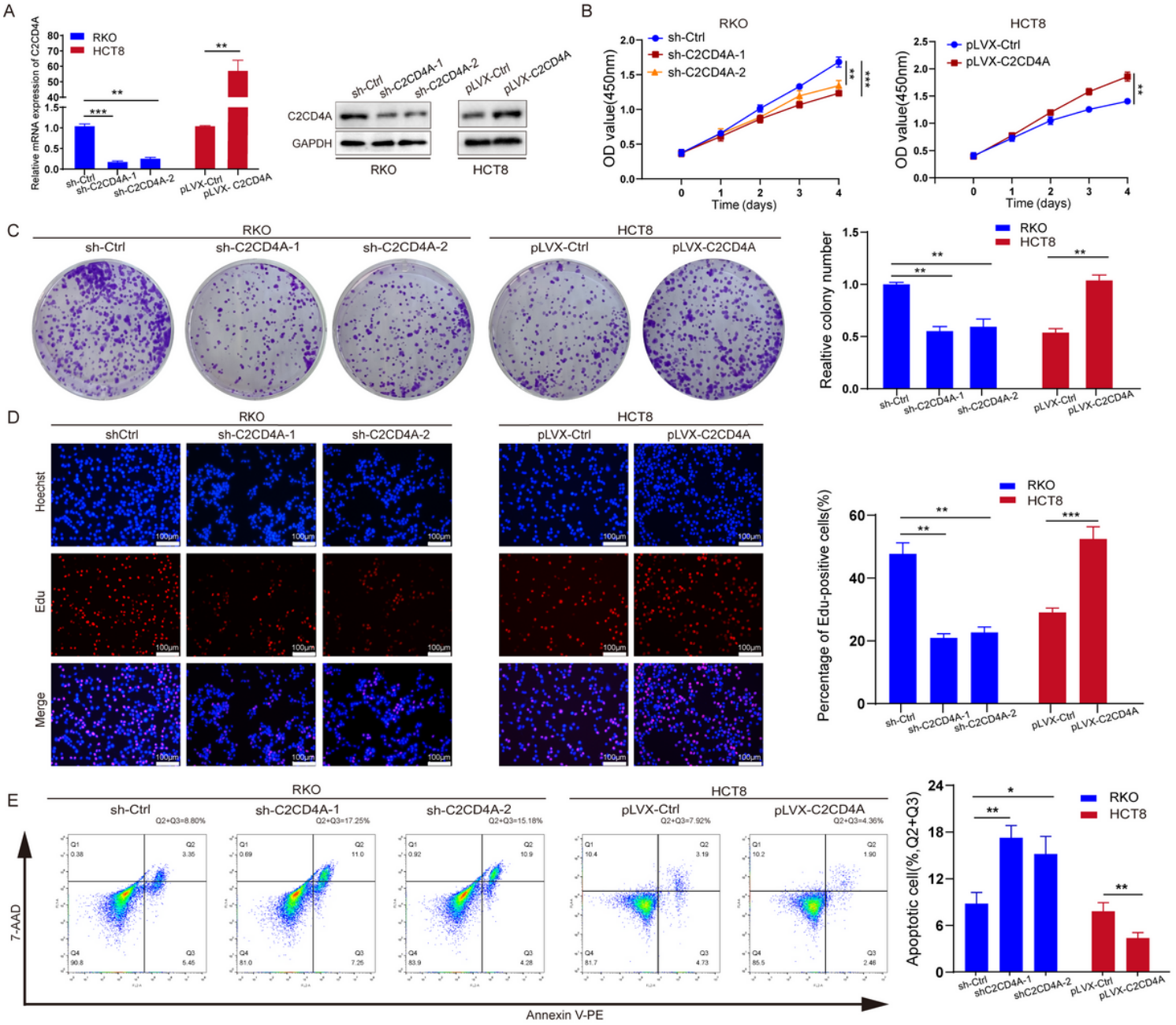

Figure 2

C2CD4A promoted CRC cell growth and proliferation in vitro. Stable RKO cells with C2CD4A knockdown and stable HCT8 cells with C2CD4A overexpression were constructed. a C2CD4A mRNA and protein expression in stable RKO and HCT8 cells were detected by qRT-PCR and western blotting. b CCK-8 assay

was used to detect the effects of downregulation and upregulation of C2CD4A in RKO and HCT8 cells. c Colony formation assay helped to detect the effects of downregulation and upregulation of C2CD4A in RKO and HCT8 cells, the representative images and quantification results are shown. d The changes in cell proliferation caused by downregulation and upregulation of C2CD4A were detected by EdU assays in RKO and HCT8 cells. e Apoptosis analysis were used to detect the effects of downregulation and upregulation of C2CD4A in RKO and HCT8 cells. Three independent experiments were performed for each group. (**P <0.01, ***P <0.001).

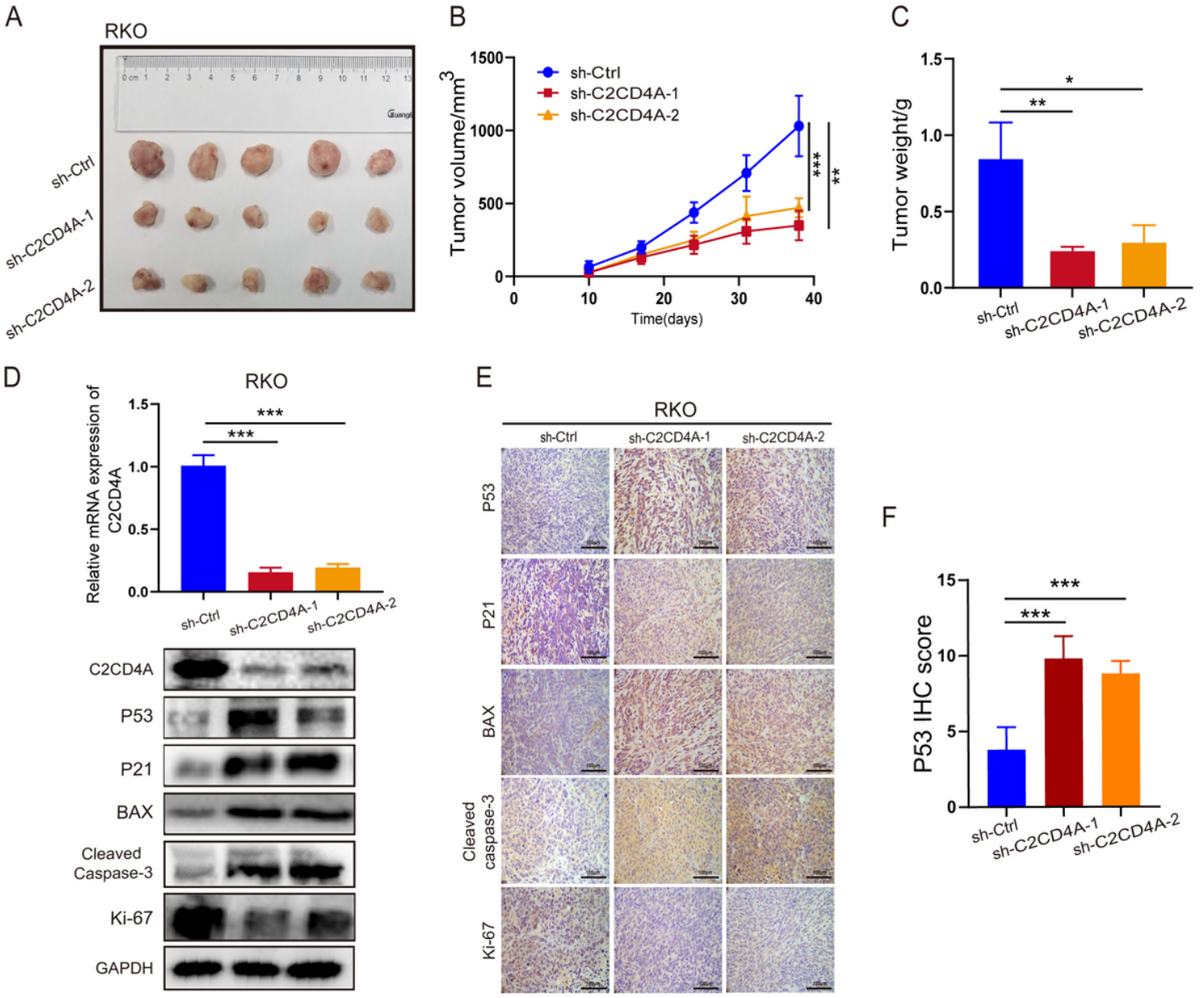

Figure 3

C2CD4A promoted CRC cell growth and proliferation in vivo. a Image of different groups subcutaneous xenograft tumors of RKO cells was shown. n=5 mice per group. b The volume of subcutaneous xenograft tumors were measured every week for five weeks. c The average final tumors weight was shown. d qRT-PCR and western blotting were performed to detect mRNA and protein level of C2CD4A in tumors. And the

protein expression levels of P53, P21, BAX, Cleaved-caspase3 and Ki-67 were shown using western blotting. e IHC staining of P53, P21, BAX, Cleaved-caspase3 and Ki-67 from the indicated tumors. f Quantification of P53 expression was determined by IHC scores. Date was shown as mean ± SD with three experiments. (*P<0.05, **P<0.01, ***P<0.001).

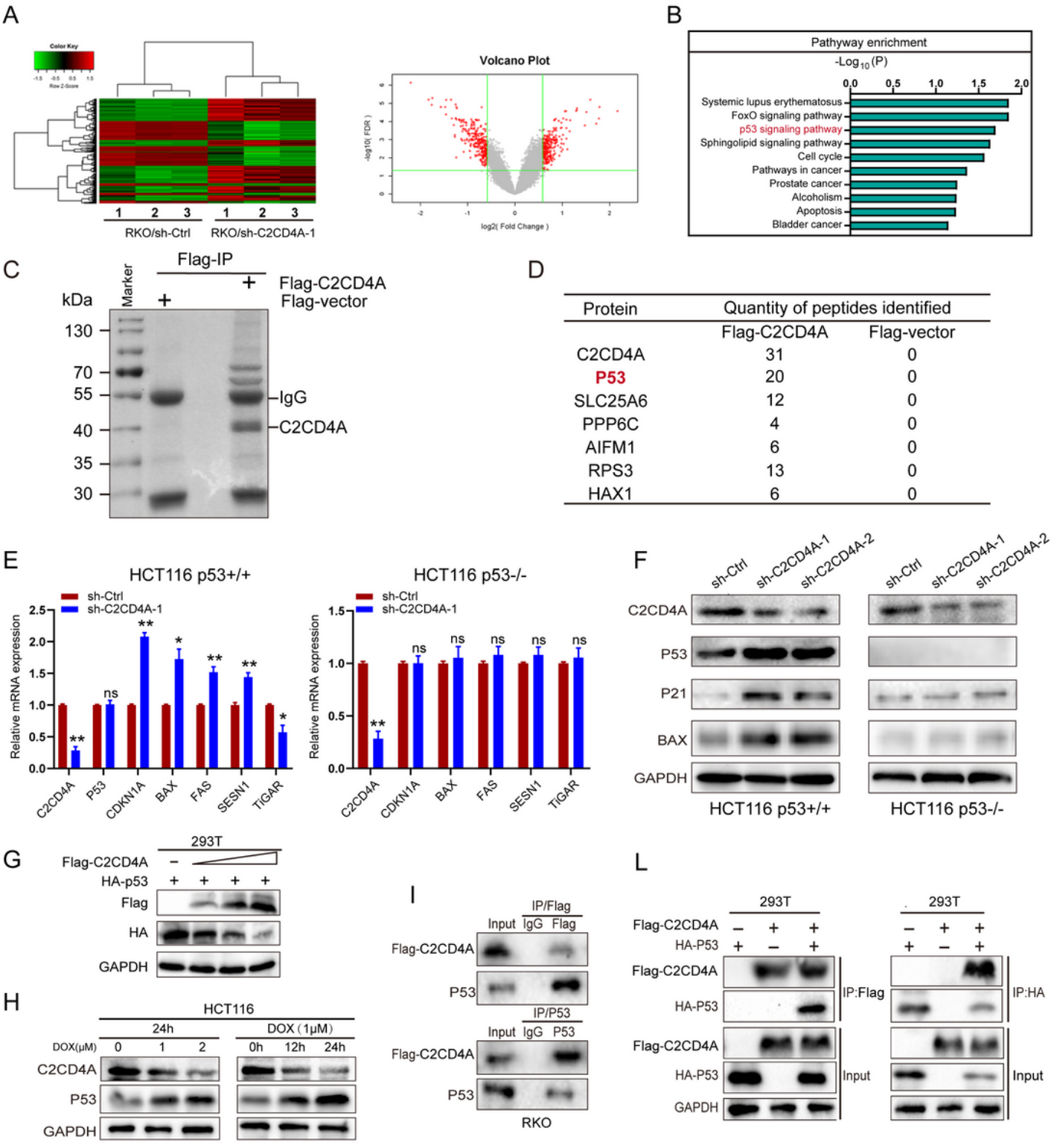

Figure 4

C2CD4A promoted CRC cells growth via P53 signaling pathway, and interacted with P53. a The heatmap and scatter diagram showed the differential expressed mRNA between RKO/sh-C2CD4A (KD-1, 2, 3) and RKO/sh-Ctrl cells (NC-1, 2, 3) screened by human cDNA microarray. b Top 10 pathways of KEGG analysis based on DEGs. c IP/MS analysis of Flag-C2CD4A-associated proteins. The Flag peptide elution was resolved on SDS-PAGE and Coomassie blue staining. d Several proteins related to cell apoptosis identified from Flag-C2CD4A IP/MS analysis. e The relative mRNA expressions of C2CD4A, P53, CDKNIA, BAX, FAS, SESN1 and TiGAR were detected using qRT-PCR. f The levels of C2CD4A, P53, CDKN1A and BAX protein expression were detected using western blotting. g 293T cells were co-transfected with Flag-C2CD4A and HA-P53 at various concentrations, and then Flag and HA expression were detected using western blotting. h HCT116 cells were treated with Dox at 1, 2 μM for 24 h, and treated at 1 μM for 12, 24 h. C2CD4A and P53 expressions were detected using western blotting. i The lysates of RKO cells were transfected with Flag-C2CD4A followed by immunoprecipitated using anti-IgG, anti-Flag or anti-P53 antibodies, and immunoprecipitation products were analyzed by western blotting with antibodies as indicated. l 293T cells were co-transfected with Flag-C2CD4A and HA-P53. Immunoprecipitation was carried out using anti-Flag or anti-HA antibody, and immunocomplexes were detected using antibodies as indicated. (ns showed no significance. *P<0.05, **P<0.01).

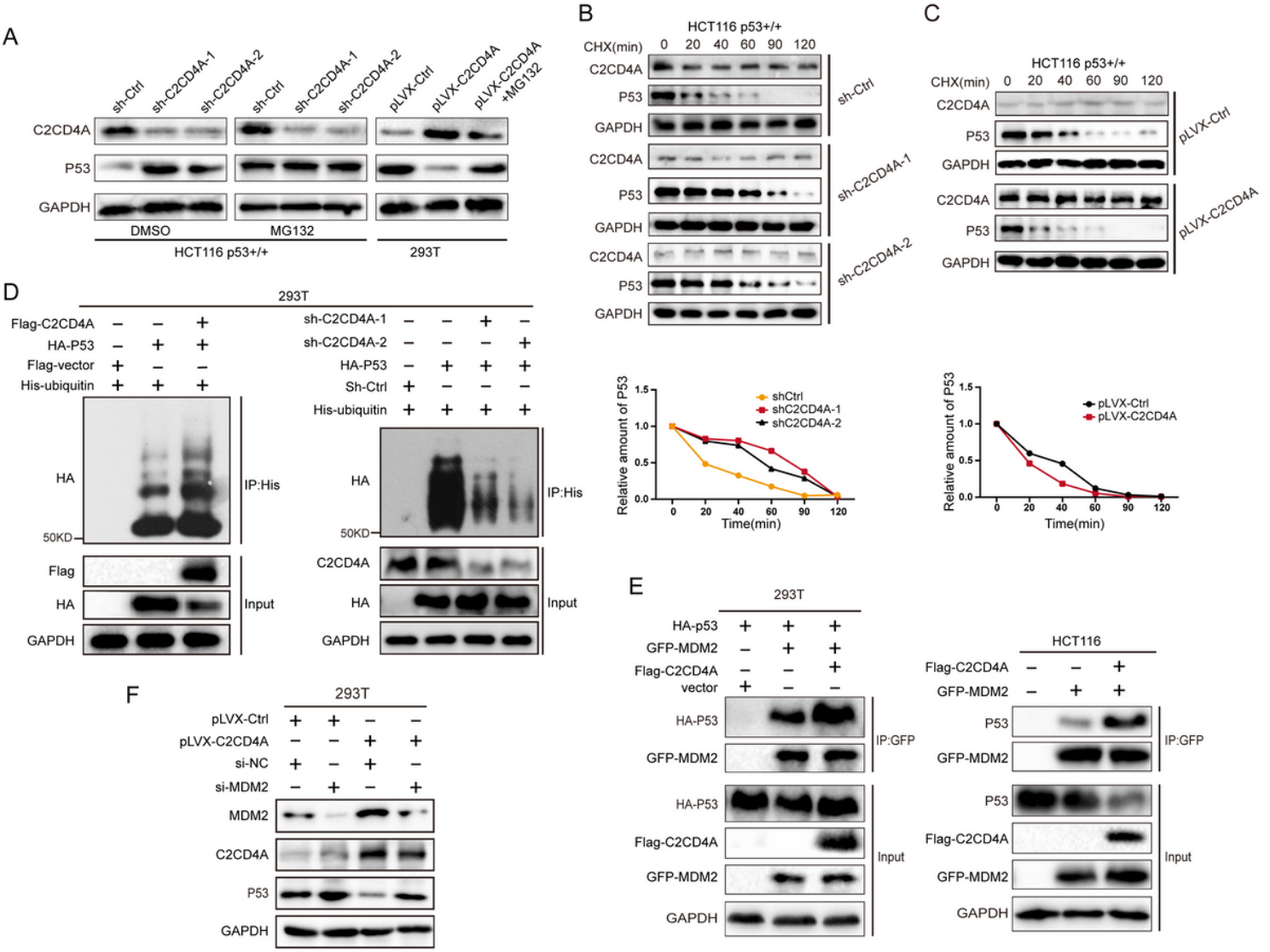

Figure 5

C2CD4A promoted ubiquitin degradation of P53 a C2CD4A-knochdown HCT116 p53+/+ cells were treated with DMSO and MG132. The treatment of DMSO served as a control. 293T cells, with stable overexpressed C2CD4A, were treated with MG132. The level of C2CD4A and P53 expression were detected using western blotting. b, c C2CD4A-knochdown HCT116 p53+/+ cells (b), C2CD4A-overexpression (c) and control HCT116 p53+/+ cells were transfected with 10 mg/mL CHX and harvested at indicated points after CHX treatment, respectively. The level of C2CD4A and P53 expression were detected using western blotting. d 293T cells were co-transfected with Flag-C2CD4A, HA-P53, His-ubiquitin or vector. His was immunoprecipitated using anti-His antibody, and P53 ubiquitination was detected using anti-HA antibody (left). 293T cells were co-transfected with His-ubiquitin, sh-C2CD4A-1, sh-C2CD4A-2, HA-P53 or vector. His was immunoprecipitated using anti-His antibody, and P53 ubiquitination was detected using anti-HA antibody (right). co-immunoprecipitation revealed the polyubiquitination of HA-P53. co-immunoprecipitation revealed the polyubiquitination of HA-P53. e 293T and HCT116 cells were co-transfected with the indicated plasmids, and Co-IP assays were performed using anti-GFP antibody to detect the interaction between P53 and MDM2. f The p53, MDM2, C2CD4A expressions were detected in the tranfected 293T cells using western blotting.

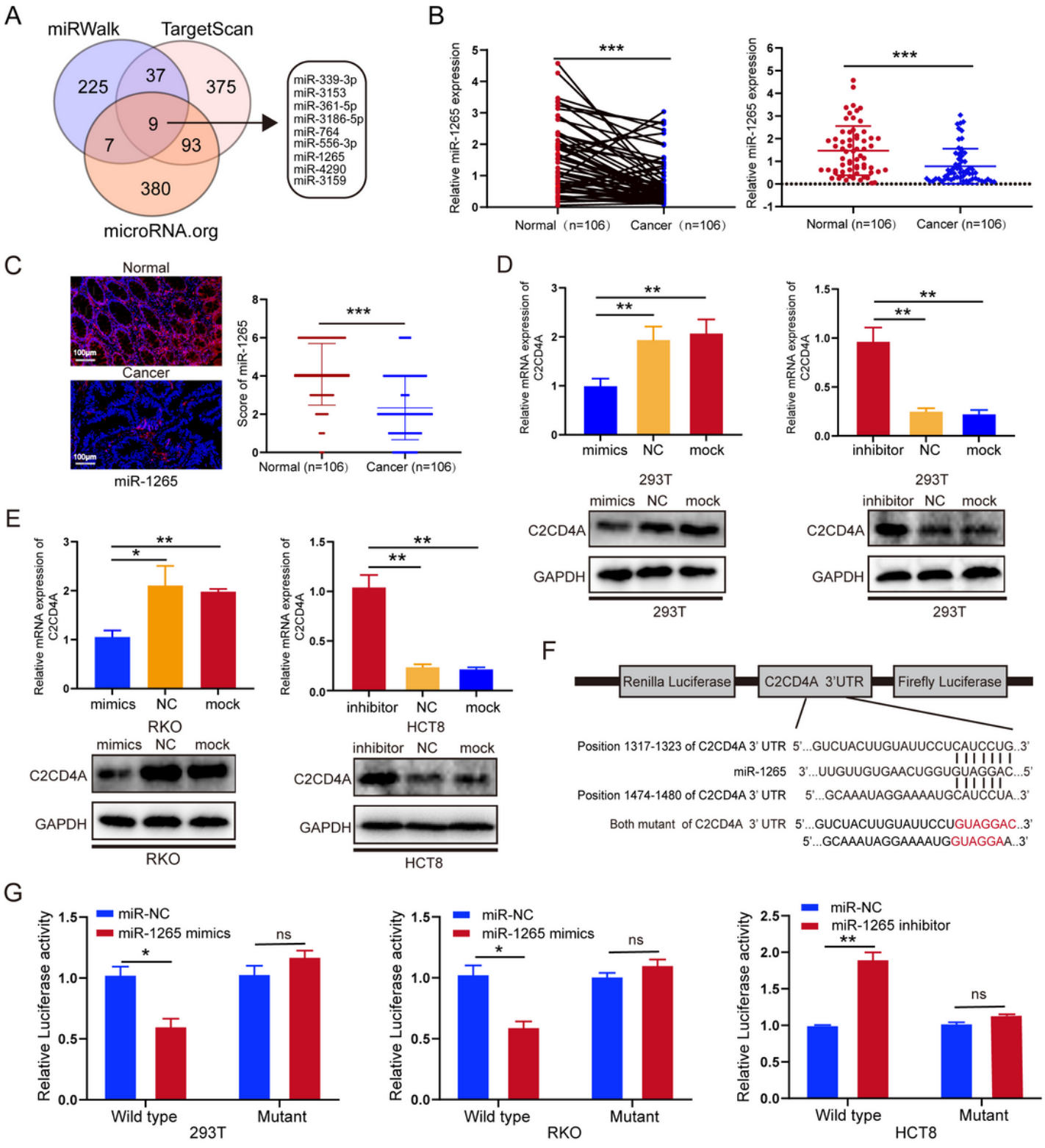

Figure 6

MiR-1265 was downregulated in CRC and suppressed C2CD4A expression by directly binding to the 3'UTR of C2CD4A mRNA. a Venn diagram illustrating the overlap of miRNAs detected in the miRWalk, TargetScan and microRNA.org. b Relative miR-1265 expression were observed to be downregulated in CRC tissues, and normalized expression of miR-1265 in 63 pairs of fresh frozen CRC tissues and adjacent noncancer tissues were detected by qRT-PCR. c The FISH results showed that the level of miR-1265 was

lower in CRC tissues than that in adjacent normal mucosae tissues from the TMA (n=106). d, e 293T, RKO, and HCT8 cells were transfected with mock, miRNA control and miR-1265 mimics or miR-1265 inhibitor, and the expression of C2CD4A were detected by qRT-PCR and western blotting. f Schematic of C2CD4A 3'UTR wild-type (WT) and mutant (Mut) luciferase reporter vector are shown. g Wild type (WT) or mutant C2CD4A 3'-UTR were transfected into 293T, RKO, HCT8 with miR-1265/NC or miR-1265 mimics or miR-1265/inhibitor. Luciferase reporter assay were performed to detect different groups luciferase activity, respectively. Mean ± SEM was shown for these data. Three independent experiments were performed for each group. (ns showed no significance. *P<0.05, **P<0.01, ***P<0.001).

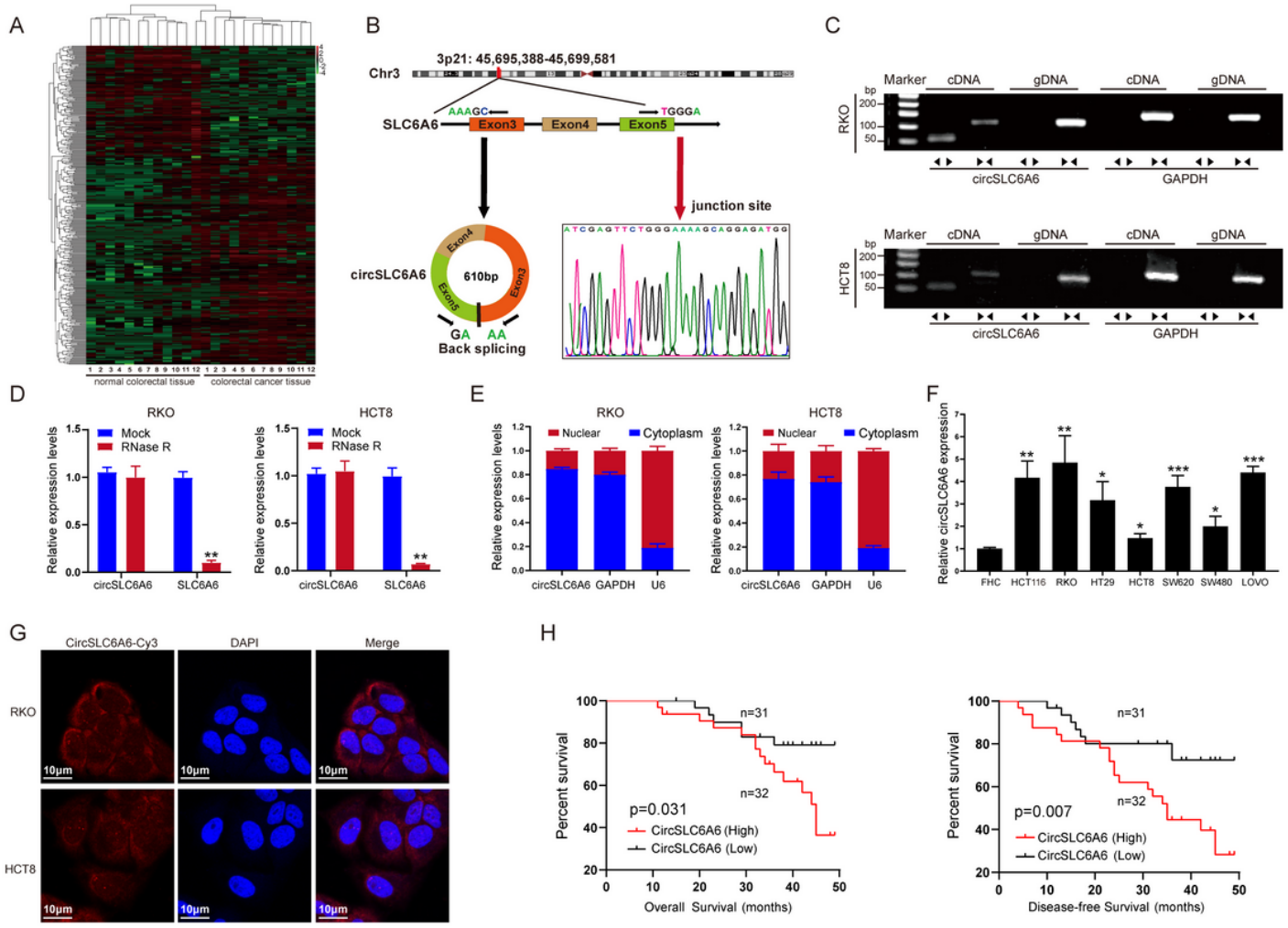

Figure 7

CircSLC6A6 is upregulated in CRC tissues and correlates with the progression and poor prognosis a The heatmap showed differentially expressed circRNAs form 12 paired fresh frozen CRC tissues in comparation with matched 12 adjacent normal mucosae tissues. b CircSLC6A6 was produced at the SLC6A6 gene locus from exons 3-5, and the head-to-tail splicing junction of circSLC6A6 was confirmed by Sanger sequencing. c Divergent primer (circSLC6A6, ◀▶) and convergent primer (SLC6A6, ▶◀) were designed. The gel electrophoresis validated the existence of circSLC6A6. Divergent primers amplified circSLC6A6 in cDNA but not gDNA in RKO and HCT8 cells. GAPDH was used as a linear control. d The relative expression of circSLC6A6 and SLC6A6 mRNA in RKO and HCT8 cells were detected by qRT-PCR

after the treatment of RNase R. e CircSLC6A6 was mainly located in the cytoplasm and determined by nuclear-cytoplasmic fractionation assay. f Relative expression of circSLC6A6 in CRC cell lines and FHC cell line were detected by qRT-PCR. g FISH assays helped to comfirmed that circSLC6A6 was mainly gathered in the cytoplasm of RKO and HCT8 cells. h Kaplan-Meier survival analysis (log-rank test) showed that CRC patients with high (32) circSLC6A6 expression were of lower OS and DFS than that of low (31) expression of circSLC6A6. Using median circSLC6A6 expression as a cutoff value. All data are presented as the mean ± SEM (**P <0.01, ***P <0.001).

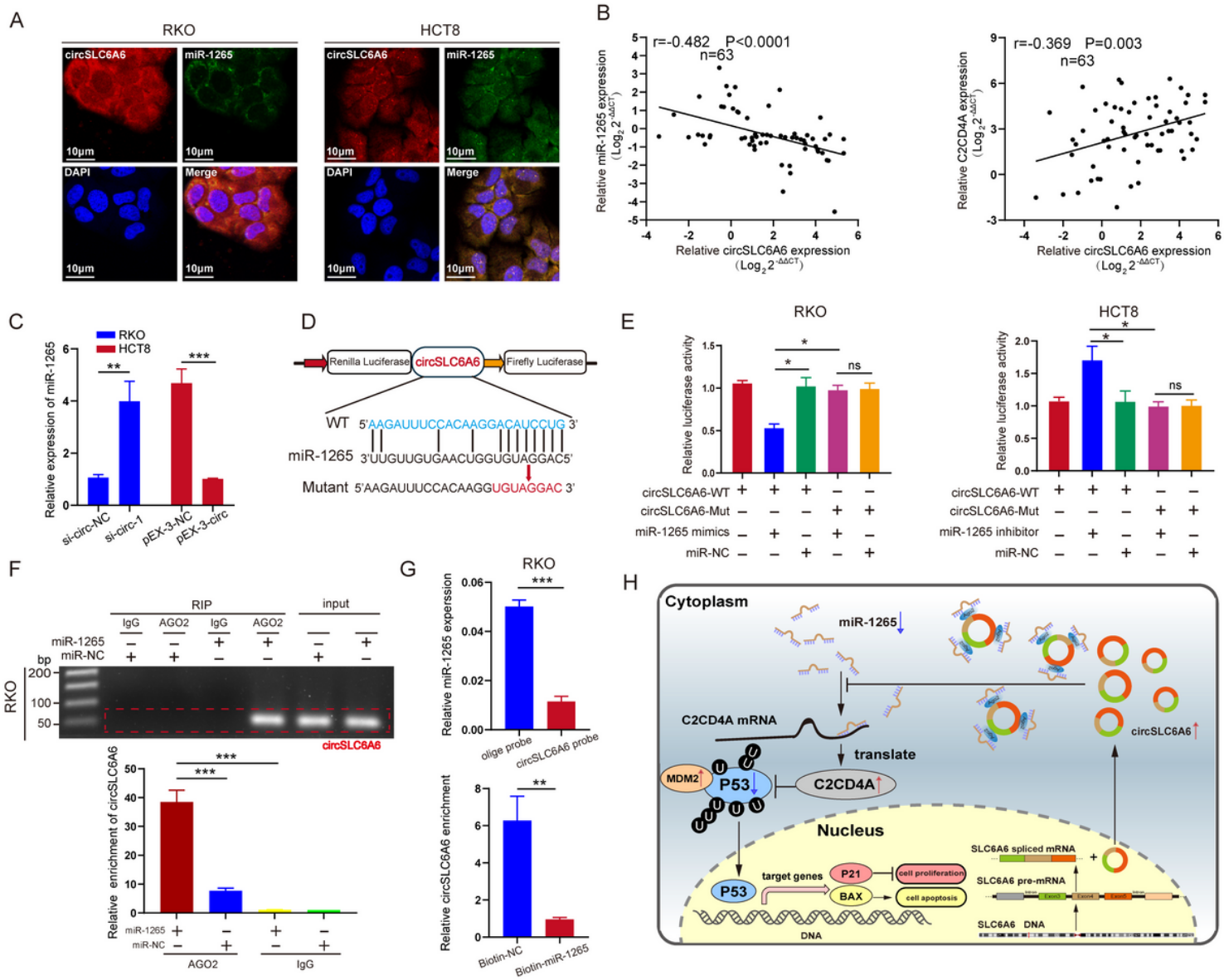

Figure 8

CircSLC6A6 functions as an efficient miR-1265 sponge, and alters the expression of C2CD4A through miR-1265 a FISH assay helped to examine the co-location between circSLC6A6 and miR-1265 in RKO and HCT8 cells. b Correlations between circSLC6A6 with miR-1265 and C2CD4A mRNA expression were performed by Pearson's correlation analysis in CRC tissue samples (n=63). c qRT-PCR was performed to test the effect of altered expression of circSLC6A6 on miR-1265p expression in RKO and HCT8 cells. d

Putative binging sites between miR-1265 and circSLC6A6 were predicted by CircInteractome, and the schematic of circSLC6A6 wild-type (WT) and mutant (Mut) luciferase reporter vectors. e Luciferase activity of circSLC6A6-WT, circSLC6A6-Mut in RKO and HCT8 after co-transfection with miR-1265 cells mimics, inhibitor or miRNA control. f Anti-Ago2 RIP was performed in RKO cells transfected with miR-1265 mimics or miR-NC, then circSLC6A6 expression detected by agarose gel electrophoresis and qRT-PCR. g In RKO cells, endogenous miR-1265 was pulled down and enriched with circSLC6A6 probe, then the enrichment of miR-1265 was detected by qRT-PCR. Biotin-miR-1265 captured endogenous circSLC6A6 in the cell complex and was compared with biotin-NC then the enrichment of circSLC6A6 was detected by using qRT-PCR. Calculation of experiment results were followed by the ratio of pull-down to input. h Proposed model for circSLC6A6/miR-1265/C2CD4A/P53 axis regulatory network, circSLC6A6 as a ceRNA for miR-1265 to regulate C2CD4A and P53 expression in CRC. All data are presented as the mean ± SEM. (ns showed no significance. *P <0.05, **P <0.01, ***P <0.001).

Supplementary Files

This is a list of supplementary files associated with this preprint. Click to download.

- Additionalfile1.docx
- Additionalfile2.docx
- Additionalfile3.docx
- Additionalfile4.docx
- Additionalfile5.docx
- Additionalfile6.docx
- Additionalfile7.docx
- Additionalfile8.docx